Copy No. 124

~~RESTRICTED~~

RM No. A6H19

A 6 H 19

6259

TECH LIBRARY KAFB, NM
0069280

RESEARCH MEMORANDUM

THE LINEAR PERTURBATION THEORY OF AXIALLY SYMMETRIC COMPRESSIBLE FLOW WITH APPLICATION TO THE EFFECT OF COMPRESSIBILITY ON THE PRESSURE COEFFICIENT AT THE SURFACE OF A BODY OF REVOLUTION

By

John G. Herriot

Ames Aeronautical Laboratory
Moffett Field, Calif.

Declassified by authority of LARC Security Classification Officer (SCO) letter dated June 16, 1983
Vincent Lommen

AFMDC
TECHNICAL LIBRARY
AFL 2811

CLASSIFIED DOCUMENT

This document contains classified information affecting the National Defense of the United States within the meaning of the Espionage Act, USC 50:31, 32. Its transmission or the revelation of its contents in any manner to an unauthorized person is prohibited by law. Information so classified may be imparted only to persons in the military and naval services of the United States, appropriate civilian officers and employees of the Federal Government who have a legitimate interest therein and to United States citizens of known loyalty and discretion who of necessity must be informed thereof.

AFMDC
TECHNICAL LIBRARY
AFL 2811

NATIONAL ADVISORY COMMITTEE
FOR AERONAUTICS

WASHINGTON
July 18, 1947

~~RESTRICTED~~

319.98/13

FILE

National Aeronautics and
Space Administration

Langley Research Center
Hampton, Virginia
23665

NASA

Reply to Attn of 139A

JUN 1 6 1983

TO: Distribution

FROM: 180A/Security Classification Officer

SUBJECT: Authority to Declassify NACA/NASA Documents Dated Prior to January 1, 1960

Effective this date, all material (informal, correspondence) classified by this Center prior to January 1, 1960, is declassified. This action does not include material derivatively classified at the Center upon instructions from other Agencies.

Immediate re-marking is not required; however, until material is re-marked by lining through the classification and annotating with the following statement, it must continue to be protected as if classified:

> "Declassified by authority of LaRC Security Classification Officer (SCO) letter dated June 16, 1983," and the signature of person performing the re-marking.

If re-marking a large amount of material is desirable, but unduly burdensome, custodians may follow the instructions contained in NHB 1640.4, subpart F, section 1203.604, paragraph (h).

This declassification action complements earlier actions by the National Archives and Records Service (NARS) and by the NASA Security Classification Officer (SCO). In Declassification Review Program #07008, NARS declassified the Center's "Research Authorization" files, which contain reports, Research Authorizations, correspondence, photographs, and other documentation. Earlier, in a 1971 letter, the NASA SCO declassified all NACA/NASA formal series documents with the exception of the following reports, which must remain classified:

Document No.	First Author
E-51A30	Nagey
E-53G20	Francisco
E-53G21	Johnson
E-53K18	Spooner
SL-54J21a	Westphal
E-55C16	Fox
E-56H23a	Himmel

JUN 2 3 1983

05-05-1987 11:28 804 864 2275 LARC TECH LIBRARY P.02

If you have any questions concerning this matter, please call Mr. William L. Simkins at extension 3281.

Jess G. Ross
2898

Distribution:
SDL 031

cc:
NASA Scientific and Technical
Information Facility
P.O. Box 8757
BWI Airport, MD 21240

NASA--NIS-5/Security
180A/RIAD
139A/TU&AO
139A/WLSimkins:elf 06/15/83 (3281)
139A/JS 6-15-83

31-01 HEADS OF ORGANIZATIONS
HESS, JANE S.,
MAIL STOP 185 BLDG 1194

05-05-1997 11:28 804 864 2375 LARC TECH LIBRARY P.03

TECH LIBRARY KAFB, NM
0069280

NACA RM No. A6H19 [redacted]

NATIONAL ADVISORY COMMITTEE FOR AERONAUTICS

RESEARCH MEMORANDUM

THE LINEAR PERTURBATION THEORY OF AXIALLY SYMMETRIC COMPRESSIBLE FLOW WITH APPLICATION TO THE EFFECT OF COMPRESSIBILITY ON THE PRESSURE COEFFICIENT AT THE SURFACE OF A BODY OF REVOLUTION

By John G. Herriot

SUMMARY

Four related methods for the study of compressible flow by means of the linear perturbation theory are discussed in detail for the case of three-dimensional flow with axial symmetry. A general method which includes the others is also discussed briefly. As an example of the application of these methods, it is shown that, for a very slender body of revolution in a uniform stream of compressible fluid, the pressure coefficient at the surface of the body is almost independent of Mach number. A more accurate result for the case of a prolate spheroid, which was given by Schmieden and Kawalki, is discussed, and it is pointed out that this result may be used to advantage for most bodies of moderate thickness. Experimental data supporting these results are given.

INTRODUCTION

Because of the high speeds of modern aircraft it is desirable to determine the effects of compressibility on the loads which may be expected on the various parts of the airplane. This determination is a problem in three-dimensional flow, but over the wing at points not too close to the tips or to the fuselage the flow approaches closely to two-dimensional flow. This fact may be used as a guide in estimating the effect of compressibility on the pressures at the wing surface. On the other hand, the fuselages of most airplanes are approximately bodies of revolution and, consequently, it is useful to know the effect of compressibility on the pressures at the surface of a body of revolution. Since the effect of compressibility on the pressure coefficient at the surface of a body of revolution is not the same as the effect on the pressure coefficient at the surface of a body in two-dimensional flow, it follows that, at points of an airplane which are close to both

[redacted]

the wing and the fuselage, the effect of compressibility must be more complex, being a combination of the effects in two-dimensional flow and in three-dimensional flow with axial symmetry. Generally, at such points, the effect of the wing on the pressure coefficient is greater than the effect of the fuselage and, consequently, the compressibility effect resembles more closely that for two-dimensional flow. On the other hand, at points of the fuselage far from the wing the flow approximates to axial flow and results appropriate to this type of flow are applicable.

For two-dimensional flow of a compressible fluid past an airfoil or other body, the Prandtl-Glauert law (references 1, 2, and 3) states that as the free-stream Mach number M increases, the pressure coefficient at the surface of the body increases according to the expression $1/\sqrt{1 - M^2}$. For bodies of small or moderate thickness and for Mach numbers below the critical, this law gives fairly satisfactory agreement with experiment, provided the departures from potential flow are not important. It has been assumed by a number of authors (references 4, 5, 6, and 7) that the same law may be applied to three-dimensional flow, but this is incorrect, as is shown in references 8 and 9 and the present report. In fact, for very slender bodies of revolution it is shown that the pressure coefficient at the surface of the body is nearly independent of the Mach number, being completely independent of the Mach number in the limiting case of zero thickness. For the case of the peak pressure coefficient (or velocity-increment ratio) at the surface of an ellipsoid of revolution, reference 9 gives a more precise result which is applicable to many bodies of moderate thickness as well as to very slender bodies.

There is a fundamental difference between the pressure-coefficient variation with Mach number in two- and three-dimensional flow. The form of the Prandtl-Glauert law which is satisfactory for bodies of moderate thickness in two-dimensional flow is independent of the thickness ratio of the body; whereas for axially symmetric flow the law for the pressure-coefficient variation depends strongly upon the thickness ratio of the body.

The Prandtl-Glauert formula for two-dimensional flow is obtained by means of the linear perturbation theory of compressible flow in which the departures of the fluid velocity from the uniform free-stream velocity are assumed small and their squares are neglected. It is clear that the theory fails in the neighborhood of a stagnation point and that elsewhere it is at best approximate, the approximation deteriorating, in the case of flow past a streamline body, as the thickness and camber of the body increase. There are a number of ways of applying this linear perturbation theory to the study of problems of compressible flow, but for any particular problem one method may be more convenient than the others. Three such general methods are described in detail in reference 4. These methods, as described in reference 4, are applicable only to two-dimensional flow.

A fourth method which is applicable to both two- and three-dimensional compressible flow is presented in reference 8. In all these methods the properties of a compressible flow are deduced by comparison with a corresponding incompressible flow whose characteristics are known. In the application of the fourth method to the problem of two-dimensional flow about a body or three-dimensional flow about a body of revolution it is necessary to take account of the fact that the bodies in the corresponding compressible and incompressible flows are of different sizes. On the other hand, in method I of reference 4, which is, unfortunately, applicable only to two-dimensional flow, the size, shape, and orientation of the body are the same in the compressible and incompressible flows. Consequently this method is more convenient for certain problems. It is pointed out in reference 4 that the other methods presented there possess certain advantages for other problems. It may be expected that methods for the study of three-dimensional compressible flow analogous to those of reference 4 will be useful and convenient for the solution of many problems. The present report describes three methods (methods I, II, and III) analogous to those of reference 4, for the study of axially symmetric compressible flow by means of the linear perturbation theory. The method of reference 8, designated method IV, is added for completeness and its relation to the other methods is pointed out. A general method which includes the others is also discussed. In method II the size, shape, and orientation of the body are the same in the compressible and incompressible flows, and consequently, this method is more convenient for certain problems. On the other hand, methods I and III may be more convenient for other problems. Great care must be exercised in using methods I, II, and III as they are applicable only to very slender bodies. Method IV is not so restricted.

If method II is applied to the problem of determining the effect of compressibility on the pressure coefficient at the surface of a very slender body of revolution, it is found that the pressure coefficient is independent of Mach number. For very slender bodies this result is in agreement with that of reference 8, in which only an ellipsoid of revolution is studied. It is instructive to obtain the same result by each of the other three methods, but, in order to do so, it is necessary to determine how the pressure coefficient at the surface of the body varies with the fineness ratio of the body in incompressible flow. It is shown in this report that, for a very slender streamline body of revolution, the pressure coefficient at the surface of the body is inversely proportional to the square of the fineness ratio. This disagrees with the result used in reference 5 but agrees with that in reference 8 for the limiting case of a very slender body. The pressure-coefficient variation for bodies of moderate thickness is also discussed.

SYMBOLS

The following symbols are used throughout this report:

p	static pressure
ρ	mass density
V	velocity
x,y,z	Cartesian coordinates
x,r,θ	cylindrical coordinates
V_x,V_y,V_z	components of velocity in x,y,z directions
V'_x	perturbation velocity in x direction $(V_x - V_o)$
V_r	radial component of velocity
a_o	velocity of sound in free stream
q	dynamic pressure $\left(\frac{1}{2}\rho V^2\right)$
P	pressure coefficient $[(p-p_o)/q_o]$
M	Mach number in free stream (V_o/a_o)
β	$\sqrt{1-M^2}$
φ	velocity potential
ψ	stream function
h,h'	radii of stream surfaces
$2l$	length of body of revolution
t	maximum radius of body of revolution
α	angle of attack
ξ,η	elliptic coordinates
$2c$	distance between foci of ellipse
a,b	semiaxes of ellipse

e eccentricity of ellipse

Subscripts and Superscripts:

o in free or undisturbed stream

i incompressible or low speed

c compressible

* at surface of body (appendix only)

THE LINEAR PERTURBATION THEORY

Consider the flow of a compressible fluid past a solid body, the undisturbed velocity of the fluid relative to axes fixed in the body being a uniform velocity V_o along the axis of x, as shown in figure 1; assume that the departures of the velocity from the undisturbed velocity V_o are small. The changes in pressure will then be small compared with the undisturbed pressure and will be proportional to the changes in density, the ratio being the square of the velocity of sound in the free stream. On a linear theory in which squares and products of small quantities are neglected, Bernoulli's equation

$$\int \frac{dp}{\rho} + \frac{1}{2} V^2 = \text{constant}$$

for steady irrotational motion becomes

$$P = \frac{p-p_o}{q_o} = \frac{p-p_o}{\frac{1}{2}\rho_o V_o^2} = -\frac{2V'_x}{V_o} \tag{1}$$

From equation (1) there is obtained

$$\frac{\rho}{\rho_o} = 1 - \frac{V_o V'_x}{a_o^2} = 1 - M^2 \frac{V'_x}{V_o} \tag{2}$$

The equation of continuity becomes

$$V_o \frac{\partial \rho}{\partial x} + \rho_o \left(\frac{\partial V_x}{\partial x} + \frac{\partial V_y}{\partial y} + \frac{\partial V_z}{\partial z} \right) = 0 \tag{3}$$

If a velocity potential φ is introduced satisfying the relations

$$\frac{\partial \varphi}{\partial x} = V_x, \quad \frac{\partial \varphi}{\partial y} = V_y, \quad \frac{\partial \varphi}{\partial z} = V_z$$

and if equation (2) is used, equation (3) becomes the familiar equation

$$\beta^2 \frac{\partial^2 \varphi}{\partial x^2} + \frac{\partial^2 \varphi}{\partial y^2} + \frac{\partial^2 \varphi}{\partial z^2} = 0 \tag{4}$$

where

$$\beta^2 = 1 - M^2 = 1 - \frac{V_o^2}{a_o^2}$$

The transformation of this equation into cylindrical coordinates x, r, θ yields

$$\beta^2 \frac{\partial^2 \varphi}{\partial x^2} + \frac{\partial^2 \varphi}{\partial r^2} + \frac{1}{r} \frac{\partial \varphi}{\partial r} + \frac{1}{r^2} \frac{\partial^2 \varphi}{\partial \theta^2} = 0 \tag{5}$$

In this report the flow is assumed to possess axial symmetry about the x-axis unless otherwise stated. In this case $\partial^2\varphi/\partial\theta^2 = 0$ and equation (5) reduces to

$$\beta^2 \frac{\partial^2 \varphi}{\partial x^2} + \frac{\partial^2 \varphi}{\partial r^2} + \frac{1}{r} \frac{\partial \varphi}{\partial r} = 0 \tag{6}$$

A stream function ψ may now be introduced writing

$$\rho V_x = \rho_o \frac{1}{r} \frac{\partial \psi}{\partial r}, \quad \rho V_r = -\rho_o \frac{1}{r} \frac{\partial \psi}{\partial x}$$

From this definition the following approximate relations are obtained:

$$\frac{1}{V_o r} \frac{\partial \psi}{\partial r} = \frac{\rho V_x}{\rho_o V_o} = \left(1 - M^2 \frac{V'_x}{V_o}\right)\left(1 + \frac{V'_x}{V_o}\right) = 1 + \beta^2 \frac{V'_x}{V_o} \tag{7}$$

$$\frac{1}{V_o r}\frac{\partial \psi}{\partial x} = -\frac{\rho V_r}{\rho_o V_o} = -\frac{V_r}{V_o} \tag{8}$$

The points for which ψ is constant constitute a surface which may be called a stream surface. The stream surface is in turn made up of streamlines.

If a solution for incompressible flow ($\beta = 1$) is known, solutions for values of β less than one may be deduced in several ways when shock waves are absent and the assumption of small departures from a uniform velocity is approximately correct.

Method I

For three-dimensional flow with axial symmetry let

$$\varphi = V_o x + f(x,r) \tag{9}$$

be a solution for the velocity potential for incompressible flow ($\beta = 1$) and let

$$\psi = \frac{1}{2}V_o r^2 + g(x,r) \tag{10}$$

be the corresponding stream function so that the following relations must hold true:

$$[1]f_x(x,r) = \frac{1}{r}g_r(x,r),\ f_r(x,r) = -\frac{1}{r}g_x(x,r) \tag{11}$$

It may be noted that $g(-\infty,r) = 0$ since the flow is undisturbed at infinity upstream. It is assumed that the limit of $g(x,r)$ as r tends to zero is finite and not zero for points x of the body not close to a stagnation point. (This assumption is correct at least for flow about a Rankine Ovoid or prolate spheroid.)

---

[1] f_x denotes the partial derivative of $f(x,r)$ with respect to x: namely, $\partial f(x,r)/\partial x$ and $f_r = \partial f/\partial r$. In equation (13) $f_r(x,\beta r)$ is the value of f_r at $(x,\beta r)$ and not the derivative of $f(x,\beta r)$ with respect to r.

Then a solution of equation (6) for $\beta < 1$ is

$$\varphi = V_o x + \frac{1}{\beta} f(x,\beta r) \tag{12}$$

The longitudinal and radial components of velocity are

$$V_x = V_o + \frac{1}{\beta} f_x(x,\beta r), \quad V_r = f_r(x,\beta r) \tag{13}$$

From equations (7), (8), and (11) it follows that

$$\frac{1}{V_o r}\frac{\partial \psi}{\partial r} = 1 + \frac{\beta}{V_o} f_x(x,\beta r) = 1 + \frac{1}{V_o r} g_r(x,\beta r)$$

and

$$\frac{1}{V_o r}\frac{\partial \psi}{\partial x} = -\frac{1}{V_o} f_r(x,\beta r) = \frac{1}{\beta V_o r} g_x(x,\beta r)$$

Then the stream function is

$$\psi = \frac{1}{2} V_o r^2 + \frac{1}{\beta} g(x,\beta r) \tag{14}$$

If the body were removed, the velocity at all points of the field would be V_o and the velocity potential and stream function would be, respectively, $V_o x$ and $\frac{1}{2}V_o r^2$. The stream surfaces would be right circular cylinders with axes along the x-axis. The effect of the body is to distort these stream surfaces. Let h denote the radius at x of a given stream surface with the body present. If the body were removed the radius of this stream surface would be h', so that $h-h'$ is the distortion of the stream surface caused by the presence of the body. If $r = h$ is substituted in equation (14) and it is observed that ψ has the same value whether the body is present or not, there is obtained

$$\psi = \frac{1}{2}V_o h^2 + \frac{1}{\beta} g(x,\beta h) = \frac{1}{2}V_o (h')^2$$

For values of h and h' which are not too small this equation yields approximately

$$h-h' = -\frac{2g(x,\beta h)}{\beta V_o(h+h')} = -\frac{g(x,\beta h)}{V_o \beta h} \qquad (15)$$

The distortion of the stream surface in the case of incompressible flow is obtained by setting $\beta = 1$ in equation (15). If the points (x,r) in the compressible flow and $(x,\beta r)$ in the incompressible flow are called corresponding points, then it is seen at once from equation (15) that at points far from the body the distortion of the stream surface in the compressible flow is the same as that at the corresponding point of the incompressible flow. To find the relation between the distortions near the body (i.e., near $r = 0$) it is only necessary to set $\psi = 0$ in equation (14). Then, since $g(x,\beta r)$ is nearly equal to $g(x,0)$ at points of a very slender body not close to a stagnation point it follows that the radius of the zero stream surface at any x in the compressible flow is $\beta^{-\frac{1}{2}}$ times the corresponding radius at the same x in the incompressible flow. It should be noted that the distortions near the body differ from those far from the body.

From equation (13) it is seen that the increase in the longitudinal velocity at any point in the compressible flow is $1/\beta$ times the increase at the corresponding point in the incompressible flow. Near the body the longitudinal velocity is nearly independent of r and consequently near $r = 0$ the longitudinal velocity increase in the compressible flow is $1/\beta$ times its value at the same point in the incompressible flow. Because of equation (1) the same relations are true for the pressure coefficient. Also from equation (13) the radial velocity at any point in the compressible flow is the same as at the corresponding point in the incompressible flow but no general comparisons can be given near $r = 0$ because the radial velocity depends upon r even for small r.

Method II

Corresponding to the solution given by equations (9) and (10) for the incompressible flow

$$\varphi = V_o x + f(x,\beta r)$$

may be written in place of equation (12) for any $\beta < 1$. The longitudinal and radial components of velocity are

$$V_x = V_o + f_x(x,\beta r), \quad V_r = \beta f_r(x,\beta r)$$

The stream function is found to be

$$\psi = \frac{1}{2}V_o r^2 + g(x,\beta r)$$

The distortion of a stream surface is approximately

$$h-h' = -\frac{2g(x,\beta h)}{V_o(h+h')} = -\frac{g(x,\beta h)}{V_o h}$$

It follows that the distortion of the stream surface at any point far from the body in the compressible flow is β times the distortion of the stream surface at the corresponding point in the incompressible flow. The radius of the zero stream surface at any x is the same in the compressible and incompressible flows or, in other words, the size, shape, and orientation of the body are the same in both flows. The pressure coefficient and the increase in the longitudinal velocity at any point in the compressible flow are the same as at the corresponding point in the incompressible flow. Near $r = 0$ the pressure coefficient and the increase in the longitudinal velocity are the same in the compressible and incompressible flows. The radial velocity at any point in the compressible flow is β times its value at the corresponding point in the incompressible flow.

It may be mentioned here that Wieselsberger (reference 10) uses a method to study compressible flow which is essentially method II of the present report, although he does not attempt to formulate any general method; however, he starts from a slightly different point of view. Instead of assuming the velocity potential to be the same at corresponding points of the compressible and incompressible flows, as done in the present report, the condition is imposed that the body shapes shall be the same in both flows and it is concluded that the velocity potentials must be the same at corresponding points.

Method III

Corresponding to the solution given by equations (9) and (10) for the incompressible flow

$$\varphi = V_o x + f(x/\beta, r)$$

may be written in place of equation (12) for any $\beta < 1$. The longitudinal and radial components of velocity are

$$V_x = V_o + \frac{1}{\beta} f_x(x/\beta,r), \quad V_r = f_r(x/\beta,r)$$

The stream function is found to be

$$\psi = \frac{1}{2}V_o r^2 + \beta g(x/\beta,r)$$

The distortion of a stream surface is approximately

$$h - h' = -\frac{2\beta g(x/\beta,h)}{V_o(h+h')} = -\frac{\beta g(x/\beta,h)}{V_o h}$$

It follows that the distortion of the stream surface near $x = x_1$ and any r in the compressible flow is β times the distortion of the stream surface near $x = x_1/\beta$ and the same r in the incompressible flow. The radius of the zero stream surface at any x in the compressible flow is $\beta^{\frac{1}{2}}$ times the corresponding radius at x/β in the incompressible flow. The pressure coefficient and the increase in the longitudinal velocity at $x = x_1$ and any r in the compressible flow are $1/\beta$ times their values at $x = x_1/\beta$ and the same r in the incompressible flow. The radial velocity at $x = x_1$ and any r in the compressible flow is the same as at $x = x_1/\beta$ and the same r in the incompressible flow.

Method IV

A fourth method, which is called an extension of the Prandtl rule, is given in reference 8. It is expressed in the following concise form:

The streamline pattern of a compressible flow to be calculated can be compared with the streamline pattern of an incompressible flow which results from the contraction of the y- and z-axes including the profile contour by the factor $\beta = \sqrt{1 - M^2}$ (x-axis in the direction of the free stream). In the compressible flow the pressure coefficient as well as the increase in the longitudinal velocity are greater in the ratio $1/\beta^2 = 1/(1-M^2)$ and the streamline slopes greater in the ratio $1/\beta = 1/\sqrt{1 - M^2}$ than those at the corresponding points of the equivalent incompressible flow.

This method is applicable to both two- and three-dimensional flow. The proof given in reference 8 differs from the proofs of methods I, II, and III given in the present report, but for the case of axially symmetric flow the methods of the present report may also be used. In this case

$$\varphi = V_o x + \frac{1}{\beta^2} f(x,\beta r)$$

is written in place of equation (12). The longitudinal and radial components of velocity are

$$V_x = V_o + \frac{1}{\beta^2} f_x(x,\beta r), \quad V_r = \frac{1}{\beta} f_r(x,\beta r)$$

The stream function is found to be

$$\psi = \frac{1}{2}V_o r^2 + \frac{1}{\beta^2} g(x,\beta r) = \frac{1}{\beta^2}\left[\frac{1}{2}V_o(\beta r)^2 + g(x,\beta r)\right]$$

From this it is seen that the points in the incompressible flow which correspond to the points of a single stream surface in the compressible flow, themselves lie on a single stream surface in the incompressible flow. In other words, if the compressible-flow field is transformed by multiplying the r-coordinate of each point by β, then stream surfaces in this field are mapped into stream surfaces in the incompressible-flow field. Thus, the two fields are entirely similar and no approximation is involved in comparing the shapes of the bodies or radii of the stream surfaces in the two flows; whereas in methods I, II, and III the comparison of the body shapes depends on an approximation and becomes exact only in the limiting case of a body of zero thickness. Thus, method IV may be expected to be the most accurate of the four methods, especailly for bodies of moderate thickness. Of course, the thickness of the body is still limited by the assumptions of the linear perturbation theory. In this connection it may be pointed out that for many problems one of the other methods may be preferable from the standpoint of convenience, but care must be exercised in their use.

General Method[1]

It is now possible to give a general method which includes the preceding methods as special cases.

Corresponding to the solution given by equations (9) and (10) for the incompressible flow a potential function

$$\varphi = V_o x + \lambda_1 f(\lambda_2 x, \lambda_3 r) \qquad (16)$$

[1]The general method as outlined in this section is due to Mr. Dean R. Chapman of the Ames Aeronautical Laboratory.

is desired. The constants $\lambda_1, \lambda_2, \lambda_3$ must be chosen so that equation (16) satisfies equation (6). If equation (16) is substituted in equation (6) and it is recalled that equation (9) satisfies equation (6) with $\beta = 1$, it is easily found that

$$\beta\lambda_2 = \lambda_3 \tag{17}$$

is a necessary and sufficient condition that equation (16) be a solution of equation (6). The longitudinal and radial components of velocity are

$$V_x = V_o + \lambda_1\lambda_2 f_x(\lambda_2 x, \lambda_3 r), \quad V_r = \lambda_1\lambda_3 f_r(\lambda_2 x, \lambda_3 r) \tag{18}$$

The stream function may be found as in method I. From equations (7), (8), (11), and (17) it follows that

$$\frac{1}{V_o r}\frac{\partial\psi}{\partial r} = 1 + \frac{\beta^2\lambda_1\lambda_2}{V_o} f_x(\lambda_2 x, \lambda_3 r) = 1 + \frac{\lambda_1\lambda_3}{\lambda_2 r V_o} g_r(\lambda_2 x, \lambda_3 r)$$

and

$$\frac{1}{V_o r}\frac{\partial\psi}{\partial x} = -\frac{\lambda_1\lambda_3}{V_o} f_r(\lambda_2 x, \lambda_3 r) = \frac{\lambda_1}{r V_o} g_x(\lambda_2 x, \lambda_3 r)$$

Then the stream function is

$$\psi = \frac{1}{2}V_o r^2 + \frac{\lambda_1}{\lambda_2} g(\lambda_2 x, \lambda_3 r) \tag{19}$$

Since any two of the three constants λ_1, λ_2, and λ_3 can be chosen arbitrarily, there is a double infinity of methods.

In general, in transforming from the compressible-flow field to the incompressible-flow field, stream surfaces are not mapped into stream surfaces. If, however, it is desired that stream surfaces map into stream surfaces, as in method IV, then an additional condition must be imposed on the λ. Equation (19) may be rewritten

$$\psi = \frac{\lambda_1}{\lambda_2}\left[\frac{1}{2}V_o(\lambda_3 r)^2\frac{\lambda_2}{\lambda_1\lambda_3^2} + g(\lambda_2 x, \lambda_3 r)\right]$$

In order that stream surfaces map into stream surfaces it is necessary and sufficient that

$$\frac{\lambda_2}{\lambda_1\lambda_3^2} = 1 \tag{20}$$

If equation (17) is used, it is seen that equation (20) can be replaced by

$$\lambda_1\lambda_2 = \frac{1}{\beta^2} \tag{21}$$

There is thus a single infinity of methods satisfying both equations (17) and (21).

If in addition it is desired to have the x-coordinate the same in both flows, it is necessary to choose $\lambda_2 = 1$ and there is then only one method satisfying both equations (17) and (21). From these equations it follows that $\lambda_1 = 1/\beta^2$ and $\lambda_3 = \beta$. This is the same as method IV which has already been discussed. It is easily seen that for methods I, II, and III equation (17) is satisfied but equation (21) is not.

It should be pointed out that great care should be exercised when using methods for which equation (21) is not satisfied. For such methods the comparison of body shapes is valid only for very slender bodies. Methods for which equation (21) is satisfied are not so restricted. It will be useful to discuss in more detail the general properties of methods for which both equations (17) and (21) are satisfied. From equations (18) and (21) it is seen that the pressure coefficient and the increase in the longitudinal velocity at any point in the compressible flow are $1/\beta^2$ times their values at the corresponding point in the incompressible flow. The thickness ratio of the body in the compressible flow is $\lambda_2/\lambda_3 = 1/\beta$ times the thickness ratio of the body in the incompressible flow. Also the streamline slopes in the compressible flow are greater in the ratio $\lambda_1\lambda_3 = 1/\beta$ than those at the corresponding points of the incompressible flow.

It may be noted that, if the general analysis is applied to two-dimensional flow, equations (17) and (21) are unaltered; however, the stream function is given by

$$\psi = V_0 y + \beta\lambda_1 g(\lambda_2 x, \lambda_3 y)$$

instead of by equation (19). It is easily seen that the methods of reference 4 satisfy equation (17) but not equation (21) and hence stream surfaces in the compressible flow do not map into stream surfaces in the corresponding incompressible flow.

VARIATION OF THE PRESSURE COEFFICIENT WITH THE FINENESS RATIO IN INCOMPRESSIBLE FLOW

It has been shown that in methods I, III, and IV the fineness ratio of the body is not the same in the compressible and incompressible flows. Consequently, in order to study the effect of compressibility on the pressure coefficient at the surface of a body of revolution by any of these methods, it is necessary to determine how the pressure coefficient at the surface of the body depends on the fineness ratio of the body in the case of incompressible flow.

Suppose the velocity potential and stream function for the flow about a slender streamline body of revolution placed in a uniform stream of incompressible fluid are, respectively,

$$\varphi = V_o x + f(x,r) \tag{22}$$

$$\psi = \frac{1}{2}V_o r^2 + g(x,r) \tag{23}$$

so that the following relations must hold true:

$$f_x(x,r) = \frac{1}{r} g_r(x,r), \quad f_r(x,r) = -\frac{1}{r} g_x(x,r)$$

As before it may be noted that $g(-\infty,r) = 0$, and again it will be assumed that the limit of $g(x,r)$ as r tends to zero is finite and not zero for points x of the body not close to a stagnation point. Then the velocity potential and stream function for the flow about a second body obtained from the first by multiplying the lateral dimensions by n are approximately

$$\varphi = V_o x + n^2 f(x,r) \tag{24}$$

$$\psi = \frac{1}{2}V_o r^2 + n^2 g(x,r) \tag{25}$$

This is easily seen by considering the stream functions of the two flows, noting that $\psi = 0$ on the bodies, and that $g(x,r)$ is approximately equal to $g(x,0)$ since r is small.

If P_1 and P_2 denote the pressure coefficients for the same x at the surfaces of the respective bodies whose radii are r_1 and nr_1, it follows from equations (1), (22), and (24) that

$$P_1 = -\frac{2(V'_x)_1}{V_o} = -\frac{2f_x(x,r_1)}{V_o}$$

$$P_2 = -\frac{2(V'_x)_2}{V_o} = -\frac{2n^2 f_x(x,nr_1)}{V_o}$$

Hence these equations give the approximate relation

$$\frac{P_2}{P_1} = \frac{(V'_x)_2/V_o}{(V'_x)_1/V_o} = \frac{n^2 f_x(x,nr_1)}{f_x(x,r_1)} = n^2 \qquad (26)$$

This approximation is valid for a very slender body since close to such a body the longitudinal velocity increase $f_x(x,r)$ is nearly independent of r. It is true that for a prolate spheroid $f_x(x,r)$ becomes logarithmically infinite but it is still true that the limit of $f_x(x,nr)/f_x(x,r)$ is unity as r tends to zero; this is sufficient to prove equation (26) for the limiting case of zero thickness.

On the other hand, the relation of equation (26) may not be the most satisfactory one for bodies of moderate thickness. Approximate expressions for the pressure coefficient and velocity increase at the surface of a prolate spheroid are given in the appendix. Let the subscript 1 refer to a prolate spheroid of thickness ratio t/l and the subscript 2 refer to a body of thickness ratio nt/l. If terms of order $(t/l)^2$ and higher are neglected in equation (A6) there is obtained

$$\frac{(P_{max})_2}{(P_{max})_1} = \frac{\left[(V'_x)_{max}\right]_2/V_o}{\left[(V'_x)_{max}\right]_1/V_o} = \frac{-(nt/l)^2 \log(nt/l)^2}{-(t/l)^2 \log(t/l)^2} = n^2\left[1 + \frac{\log n^2}{\log(t/l)^2}\right] \qquad (27)$$

If terms of order $(t/l)^2$ are retained but terms of higher order are neglected in equation (A6) there is obtained

$$\frac{(P_{max})_2}{(P_{max})_1} = \frac{\left[(V'_x)_{max}\right]_2/V_o}{\left[(V'_x)_{max}\right]_1/V_o} = \frac{-\frac{1}{2}(nt/l)^2\log(nt/l)^2 - (1-\log 2)(nt/l)^2}{-\frac{1}{2}(t/l)^2\log(t/l)^2 - (1-\log 2)(t/l)^2}$$

$$= n^2\left[1 + \frac{\log n^2}{\log(t/l)^2 + 2\,(1-\log 2)}\right] \qquad (28)$$

In applying these relations to the study of compressible flow by means of method IV it will be necessary to take n equal to β. Corresponding to a Mach number of 0.8, β is 0.6. With $n = 0.6$ the approximations given in equations (27) and (28), as well as the true values of the left members for a prolate spheroid, are plotted as a function of t/l in figure 2. In addition this ratio is plotted in figure 2 for the NACA 111 series (reference 11) of bodies as well as for a series of bodies given in reference 12. Unfortunately these series of bodies are not related to one another so that one body may be obtained from another of the series by multiplication of the radii by a fixed factor. However, the distortion is not great. Straight lines corresponding to $n = 0.6$ and $n^2 = 0.36$ are added to figure 2 for comparison. It appears that for small values of t/l equation (28) gives the best approximation for the prolate spheroid; whereas for large values of t/l equation (27) is better, but neither is of much value for values of t/l in excess of 0.30. The approximation given by equation (28) appears to be most satisfactory for general use but its application should be restricted to bodies whose thickness ratios are less than 0.30. It should be noted that as t/l tends to zero the right members of equations (27) and (28) both reduce to n^2 in agreement with equation (26).

VARIATION OF PRESSURE COEFFICIENT WITH MACH NUMBER IN COMPRESSIBLE FLOW

Consider a slender streamline body of revolution of length $2l$ and maximum radius t in a uniform stream of compressible fluid. Suppose that the undisturbed fluid flows in the direction of the positive x-axis and that the body is placed with its axis along the x-axis and its center

at the origin as shown in figure 1. Denote by P_c the pressure coefficient at any point x of the surface of the body. Let P_i be the pressure coefficient at the same point of the surface of the same body under the assumption that the fluid is incompressible.

Method II is the most convenient method to use, for the size, shape, and orientation of the body are unchanged in the corresponding incompressible flow. It follows at once that $P_c = P_i$ or, in other words, that the pressure coefficient is independent of the Mach number.

In using any of the other methods, it is necessary to take account of the change in the shape of the body in passing from the compressible flow to the corresponding incompressible flow. Since methods I and III are valid only for very slender bodies the appropriate pressure-coefficient variation with thickness is given by equation (26). When method I is used, the corresponding body in the incompressible flow is of length $2l$ and maximum radius $t\beta^{\frac{1}{2}}$ so that $P_c = (1/\beta)(\beta P_i) = P_i$. Again, if method III is used, the body in the incompressible flow is of length $2l/\beta$ and maximum radius $t\beta^{-\frac{1}{2}}$ so that the thickness ratio is decreased in the ratio $\beta^{\frac{1}{2}}$. It follows that $P_c = (1/\beta)(\beta P_i) = P_i$. Finally when method IV is used the body in the incompressible flow is of length $2l$ and maximum radius $t\beta$ so that $P_c = (1/\beta^2)(\beta^2 P_i) = P_i$.

Methods I, II, and III are valid only for very slender bodies not only because some distortion is introduced in the comparison of the body shapes but also because the slight variation of the pressure coefficient with distance from the axis of the body is neglected when this distance is small. This variation with distance must be considered in order to avoid inconsistent results if the closer approximations of equations (27) and (28) are used in conjunction with methods I, II, and III. Since this is inconvenient to do and since method IV is not subject to these limitations, it is preferable to use the latter method when the closer approximations given by equations (27) and (28) are used.

If equation (27) is used together with method IV it is easily found that

$$\frac{(P_{max})_c}{(P_{max})_i} = \frac{\left[(V'x)_{max}\right]_c/V_0}{\left[(V'x)_{max}\right]_i/V_0} = 1 + \frac{\log \beta^2}{\log(t/l)^2} \tag{29}$$

whereas, if equation (28) is used, there is obtained

$$\frac{(P_{max})_c}{(P_{max})_i} = \frac{\left[(V'x)_{max}\right]_c/V_0}{\left[(V'x)_{max}\right]_i/V_0} = 1 + \frac{\log \beta^2}{\log(t/l)^2 + 2(1-\log 2)} \tag{30}$$

Equation (29) is the result of reference 8 and equation (30) is the asymptotic first approximation of reference 9. The result of equation (30) is shown graphically in figure 3.

Figure 2 shows that equation (30) is likely to be most suitable for general use although for thicker prolate spheroids equation (29) would appear to be better. Neither of these equations should be used for bodies whose thickness ratios exceed 0.30. For thicker bodies the more exact results of reference 9 may be used. For very slender bodies the right members of both equations (29) and (30) reduce to unity in agreement with the result previously obtained. In the application of equation (30) to bodies other than prolate spheroids, t/l may be chosen as the actual thickness ratio of the body or as the thickness ratio of the spheroid having the same peak pressure coefficient as the body, or t/l may be chosen in some other appropriate manner. This uncertainty in the choice of t/l will not materially affect the results obtained from equation (30).

References 8 and 9 study only the maximum velocity increment, but if equations (A9) and (A10) of the appendix are used, and terms of order $(t/l)^2$ are retained, then it is easily shown that at the surface of a spheroid

$$\frac{(V'_x)_c/V_o}{(V'_x)_i/V_o} = 1 + \frac{\log \beta^2}{\log(t/l)^2 + 2\left\{[1-(x/l)^2]-\log 2\right\}} \tag{31}$$

$$\frac{P_c}{P_i} = 1 + \frac{\log \beta^2}{\log(t/l)^2 + (x/l)^2/[1-(x/l)^2] + 2 - 2\log 2} \tag{32}$$

It should be noted that in contrast to equation (26) P_c/P_i and $[(V'_x)_c/V_o]/[(V'_x)_i/V_o]$ are slightly different because terms of higher order have been retained. Of course equations (31) and (32) are valid only over the central portion of the spheroid and are invalid near the stagnation points. When $x = 0$ equations (31) and (32) reduce to equation (30). Generally it will be sufficiently accurate to use equation (30) in place of equations (31) and (32).

ESTIMATION OF CRITICAL MACH NUMBERS

The critical Mach number of any body can be determined from its low-speed peak pressure coefficient provided the variation of peak pressure coefficient with Mach number is known. If equation (30) is

used to estimate this variation for a body of revolution and if in this equation t/l is chosen as the thickness ratio of the prolate spheroid having the same peak pressure coefficient as the body under consideration, then the solid curve of figure 4 is obtained. If the law for very slender bodies is used, namely, that the pressure coefficient is independent of Mach number, the dashed curve of figure 4 is obtained. The curves applicable to two-dimensional flow obtained from the Prandtl-Glauert and Kármán-Tsien (reference 5) laws are shown for comparison.

EXPERIMENTAL RESULTS AND DISCUSSION

In order to determine whether the results of the present paper are in agreement with experiment, a considerable amount of experimental pressure data was studied. The fuselages of many airplanes are approximately bodies of revolution but most data have been taken with the wing on the fuselage. At stations near the wing the pressure coefficient is more influenced by the presence of the wing than it is by the fuselage. Consequently, data on the fuselage without the wing or on the fuselage far from the wing are needed.

Pressure data for a fuselage without a wing or other protuberances were available for only one airplane which, in this report, is designated as airplane A. These data were taken in the Ames 16-foot high-speed wind tunnel and corrected for tunnel-wall effects, the correction to the Mach number being in the neighborhood of 5 percent. This fuselage is a body of revolution. Back of the maximum section, the regular fuselage was replaced by a conical shape as shown in figure 5. The length of the model tested was 135.0 inches and the maximum thickness was 37.56 inches, giving a fineness ratio of 3.595. The locations of the pressure orifices are also shown in figure 5. The model was supported in the tunnel by means of two struts connected to it about 45° on either side of the bottom vertical center line of the fuselage. Since the data from the lower orifices might be influenced by these struts, the variation of pressure coefficient with Mach number is shown in figure 6 only for the orifices on or near the top of the model. The data of orifices T-2 and T-3 may be influenced by the presence of two holes in the fuselage near the nose which were to simulate gun ports. For purposes of comparison a $1/\beta$ curve is added in each case. For orifices T-7, TR-7, T-8, and TR-8 a curve showing the theoretical variation of the peak pressure coefficient as given by equation (30) is added. This curve is seen to lie very close to the $1/\beta$ curve appropriate to two-dimensional flow. It can be seen that for the orifices T-7, TR-7, T-8, and TR-8 the experimental pressure coefficients rise slightly with Mach number but less than predicted theoretically by equation (30). At the other orifices the pressure coefficient rises less rapidly and even falls at some of the orifices, changing sign in one or two cases. This is not predicted by the linear theory

at all. A more accurate and detailed calculation carried out in reference 13 for a particular body, however, reveals such behavior on some parts of the body.

The other available data were for a fuselage with wing. It was considered that pressure data for orifices near the nose of a long fuselage would be little affected by the presence of the wing. Near the wing, the effect of the wing would be predominant.

Figure 7 shows the forward portion of the fuselage of airplane B together with the position of the wing. The fuselage is nearly a body of revolution, but the upper surface is complicated by the presence of the pilot's windshield; whereas the lower surface differs from the regular shape only by having a flat bombardier's window very near the nose. The locations of five pressure orifices on the lower surface of the fuselage on its vertical center line are also shown. These orifices are all to the rear of the bombardier's window on that portion of the fuselage which approximates most closely to a body of revolution. Figure 8 shows the variation of pressure coefficient with Mach number at these five orifices. These data were taken in the Ames 16-foot high-speed wind tunnel and were not corrected for tunnel-wall effects. It is seen that at those orifices farthest from the nose the pressure coefficient is remarkably constant as the Mach number is changed.

Figure 9 shows the fuselage, wing, and canopy of a 1/5-scale model of airplane C together with the locations of some of the pressure orifices. The forward portion of this fuselage is approximately a body of revolution, the nose duct having been replaced by a plug. Figure 10 shows the variation of the pressure coefficient with Mach number at a number of orifices, the data having been taken for the wing and basic fuselage but with the canopy removed. A number of orifices are not shown in figure 9 as it is drawn with the canopy on. But the position of each orifice for which data are given in figure 10 is described by giving its distance in inches from the nose of the fuselage with plug. These data were obtained in the Langley 8-foot high-speed wind tunnel. It is seen that, at those orifices which are well forward of the wing, the pressure coefficient is nearly constant or increases slowly with increasing Mach number, its curve remaining below the $1/\beta$ curve; but near the wing the increase of the pressure coefficient is much more rapid and at several orifices the increase is more rapid than $1/\beta$. At such orifices the effect of the wing is greater than that of the fuselage. Moreover the flow over the wing is more nearly two-dimensional and so the $1/\beta$ law would be expected to hold. The critical Mach number of the wing is 0.68 and this may account for the drops in some of the curves above $M = 0.70$.

It was considered that in the cases of airplanes B and C the bodies tested did not resemble pure bodies of revolution sufficiently closely to warrant a comparison of the test results with the theoretical results of equation (30).

The Kollsman pitot-static tube F.S.S.C. No. 88-T-2950 is shown in figure 11. This tube is a body of revolution, and a short distance back of the nose its cross section remains constant for a considerable distance, the diameter of this constant portion being seven-eighth inch. The static orifices are located near the center of this length of constant cross section and are 5-1/16 inches from the nose. Figure 12 shows the variation of pressure coefficient with Mach number at the static orifices of this pitot-static tube. These data were obtained in the calibration of this instrument in the Ames 1- by 3½-foot high-speed wind tunnel and corrected for the effect of tunnel blockage. The tunnel choked at a Mach number of 0.952 and at Mach numbers close to this value the tunnel corrections are unreliable. For this reason the sharp drop in the curve occurring at Mach numbers over 0.9 should be disregarded. For purposes of comparison a $1/\beta$ curve was added to figure 12 as well as a straight line to indicate the theory of the present report for very slender bodies. In addition, a curve has been added showing the variation of peak pressure coefficient as predicted by equation (30) for a body of fineness ratio 20, this being the fineness ratio which appears appropriate to the model tested. It is seen that the pressure coefficient is nearly constant increasing only very slowly with increasing Mach number. The increase is very small and is not far from that predicted by equation (30) but is far below $1/\beta$.

The pressure distribution on the fuselage of a midwing airplane has been studied by Delano. (See reference 14.) It was found that the peak negative pressures on the fuselage occurred near the wing and were more dependent on the wing than on the fuselage. The variation of these peak pressures was in good agreement with the $1/\beta$ law, but at other points on the fuselage the pressure-coefficient variation does not follow this law. These conclusions are in agreement with the data shown in figure 10. It appears that near the wing where the peak pressures occur, the flow is nearly two-dimensional and the $1/\beta$ law gives a good picture of the actual variation of the pressure coefficient. But at points farther from the wing the flow is more nearly three-dimensional and at such points which are not too close to a stagnation point the pressure coefficient should be constant at least for very slender bodies according to the theory developed in this report. For somewhat thicker bodies the pressure coefficient may rise slowly with increasing Mach number and equation (30) gives a formula for this increase. The experimental data of Delano show several different types of pressure-coefficient variation. The type may depend on the proximity of the wing and may result from wing and fuselage pressures following different laws of variation.

It is assumed by Robinson and Wright (reference 6) that the variation of the peak pressure coefficient with Mach number can best be represented by the $1/\beta$ law for three-dimensional flow as well as for two-dimensional flow. In view of the foregoing discussion this would appear to be justified, provided the peak pressure coefficient occurs near the wing, and

this is usually the case at least for a wing and fuselage combination. No attempt is made in reference 6 to predict the pressure-coefficient variation at points other than where the peak occurs.

It appears that, for those bodies which approximate closely to bodies of revolution and for points not too close to a stagnation point, the pressure coefficient is nearly constant or increases slowly with Mach number. It cannot be said that the pressure coefficient is exactly constant in all cases, as proved in this report for a very slender body of revolution. Nevertheless equation (30) appears to overestimate the actual increase for the true bodies of revolution tested.

CONCLUSIONS

1. Four related methods and a general method for the study of three-dimensional axially symmetric compressible flow by means of the linear perturbation theory are presented. In each case the properties of the compressible flow are obtained from those of a corresponding incompressible flow. Each of the methods possesses certain advantages over the others. For example, in method II the body shape, size, and orientation are the same in the corresponding incompressible flow as in the compressible flow; whereas in method IV the streamline fields are entirely similar, the incompressible field being obtained by a contraction of the compressible field in the radial direction. Methods I, II, and III are limited to very slender bodies; whereas method IV may be applied to bodies of moderate thickness.

2. By means of each of these four methods, it is found that the pressure coefficient at the surface of a very slender streamline body of revolution placed in a uniform stream of compressible fluid is nearly independent of the Mach number, being entirely independent of the Mach number in the limiting case of zero thickness. This result is invalid near a stagnation point and its application is therefore usually limited to the central portion of the body. For a prolate spheroid the variation of the peak pressure coefficient with Mach number is given by the formula

$$\frac{(P_{max})_c}{(P_{max})_i} = 1 + \frac{\log(1-M^2)}{\log(t/l)^2 + 2(1-\log 2)}$$

and this result may be used for bodies of moderate thickness (thickness ratio less than 0.30). For very slender bodies the second term is negligible while for a thickness ratio of 0.2 the increase in the pressure coefficient is about half that for a two-dimensional body.

3. Experimental data for bodies of revolution without wings or other protuberances show nearly constant or slowly rising pressure coefficient as the Mach number increases. The rise is usually less than that predicted by equation (30). Experimental data for bodies of revolution with wings show nearly constant or slowly rising pressure coefficient far from the wing but rapidly rising pressure coefficient near the wing, the rise agreeing with that predicted for two-dimensional bodies.

4. On the fuselage of an airplane near the wing the pressure coefficient is influenced more by the wing than by the fuselage and, at such points, the pressure-coefficient variation is best represent by the $1/\sqrt{1 - M^2}$ law appropriate to two-dimensional flow. Since the peak pressure coefficient usually occurs near the wing, the variation of peak pressure coefficient for a wing-fuselage combination is best represented by the $1/\sqrt{1 - M^2}$ law. On the other hand, at points on the fuselage far from the wing and not close to a stagnation point the pressure coefficient is nearly constant. In order to obtain an estimate of the rise in the pressure coefficient, the result for the peak pressure coefficient given by equation (30) may be used.

Ames Aeronautical Laboratory,
National Advisory Committee for Aeronautics,
Moffett Field, Calif., May 13, 1946.

APPENDIX

PROLATE SPHEROID – INCOMPRESSIBLE FLOW

Consider a prolate spheroid immersed in a uniform stream of incompressible fluid whose velocity at a large distance from the body is V_o in the direction of the positive x-axis. Suppose the spheroid to be located with its center at the origin and its major axis along the x-axis. Let c denote the distance of either focus from center of spheroid and ξ, η denote the elliptic coordinates for a meridian section, so that the following relations between the coordinates are satisfied:

$$x = c \cosh \xi \cos \eta$$

$$r = c \sinh \xi \sin \eta$$

Also let

$a = c \cosh \xi^* =$ semimajor axis of ellipse forming meridian section

$b = c \sinh \xi^* =$ semiminor axis of ellipse forming meridian section

$e = \sqrt{1 - (b/a)^2} = \frac{c}{a} = \frac{1}{\cosh \xi^*} =$ eccentricity of ellipse forming meridian section

where ξ^* is the value of ξ on the ellipse forming meridian section. Then the velocity potential for this flow is given in section 105 of Lamb's Hydrodynamics (reference 15) in the form

$$\varphi = V_o x - \frac{2V_o c}{\log \frac{1+e}{1-e} - \frac{2e}{1-e^2}} \cos \eta \left\{ \frac{1}{2} \cosh \xi \log \frac{\cosh \xi + 1}{\cosh \xi - 1} - 1 \right\} \qquad (A1)$$

If the equations which give x and r in terms of ξ and η are differentiated partially with respect to x and r, it is found that

$$\frac{\partial \xi}{\partial x} = \frac{\partial \eta}{\partial r} = \frac{\sinh \xi \cos \eta}{c(\cosh^2 \xi - \cos^2 \eta)}$$

$$\frac{\partial \xi}{\partial r} = -\frac{\partial \eta}{\partial x} = \frac{\cosh \xi \sin \eta}{c(\cosh^2 \xi - \cos^2 \eta)}$$

The velocity component in the direction of the x-axis is given by

$$V_x = \frac{\partial \varphi}{\partial x} = \frac{\partial \varphi}{\partial \xi}\frac{\partial \xi}{\partial x} + \frac{\partial \varphi}{\partial \eta}\frac{\partial \eta}{\partial x}$$

When equation (A1) is used, it is easily found that

$$V_x = V_o - \frac{V_o}{\log\frac{1+e}{1-e} - \frac{2e}{1-e^2}}\left\{\log\frac{\cosh\xi + 1}{\cosh\xi - 1} - \frac{2\cosh\xi}{\cosh^2\xi - \cos^2\eta}\right\} \tag{A2}$$

Similarly, the radial velocity component is given by

$$V_r = \frac{\partial \varphi}{\partial r} = \frac{\partial \varphi}{\partial \xi}\frac{\partial \xi}{\partial r} + \frac{\partial \varphi}{\partial \eta}\frac{\partial \eta}{\partial r}$$

and it is easily found that

$$V_r = \frac{2V_o \sin\eta\cos\eta}{\left(\log\frac{1+e}{1-e} - \frac{2e}{1-e^2}\right)\left(\cosh^2\xi - \cos^2\eta\right)\sinh\xi} \tag{A3}$$

At the surface of the spheroid equations (A2) and (A3) reduce to

$$\frac{V_x^*}{V_o} = 1 - \frac{\log\frac{1+e}{1-e} - \frac{2e}{1-e^2\cos^2\eta}}{\log\frac{1+e}{1-e} - \frac{2e}{1-e^2}} \tag{A4}$$

$$\frac{V_r^*}{V_o} = \frac{2ae^3\sin\eta\cos\eta}{\left(\log\frac{1+e}{1-e} - \frac{2e}{1-e^2}\right)\left(1-e^2\cos^2\eta\right)b} \tag{A5}$$

It follows that

$$\lim_{b/a \to 0} \frac{V_x^*/V_0 - 1}{(b/a)^2 \log(b/a)^2}$$

$$= -\lim_{e \to 1} \frac{\log(1+e) - \log(1-e) - \dfrac{2e}{1-e^2\cos^2\eta}}{(1-e^2)\log(1-e^2)[\log(1+e) - \log(1-e)] - 2e\log(1-e^2)}$$

$$= -\lim_{e \to 1} \frac{-1 + \dfrac{1}{\log(1-e)}\left\{\log(1+e) - \dfrac{2e}{1-e^2\cos^2\eta}\right\}}{-2e + \dfrac{1}{\log(1-e)}\left\{(1-e^2)[\log^2(1+e) - \log^2(1-e)] - 2e\log\left(\frac{1+e}{1-e}\right)\right\}}$$

$$= -\frac{1}{2}$$

unless $\eta = 0$ or π. Also

$$\lim_{b/a \to 0} \frac{V_x^*/V_0 - 1 + \frac{1}{2}(b/a)^2 \log(b/a)^2}{(b/a)^2}$$

$$= \lim_{e \to 1} \frac{-\log\dfrac{1+e}{1-e} + \dfrac{2e}{1-e^2\cos^2\eta} + \frac{1}{2}(1-e^2)\log(1-e^2)\log\dfrac{1+e}{1-e} - e\log(1-e^2)}{(1-e^2)[\log(1+e) - \log(1-e)] - 2e}$$

$$= \lim_{e \to 1} \frac{(1-e)\log(1-e) + \frac{1}{2}(1-e^2)\log(1-e^2)\log\dfrac{1+e}{1-e} - (1+e)\log(1+e) + \dfrac{2e}{1-e^2\cos^2\eta}}{(1-e^2)[\log(1+e) - \log(1-e)] - 2e}$$

$$= \frac{-2\log 2 + 2\csc^2\eta}{-2}$$

$$= \log 2 - \csc^2\eta$$

unless $\eta = 0$ or π. If terms of higher order than $(b/a)^2$ are neglected it follows that, except for $\eta = 0$ or π,

$$\frac{V_x^*}{V_o} = 1 - \frac{1}{2}\left(\frac{b}{a}\right)^2 \log\left(\frac{b}{a}\right)^2 - (\csc^2 \eta - \log 2)\left(\frac{b}{a}\right)^2 \qquad (A6)$$

In the same way it follows that

$$\lim_{b/a \to 0} \frac{V_r^*/V_o}{b/a} = \lim_{e \to 1} \frac{2e^3 \sin \eta \cos \eta}{(1-e^2\cos^2 \eta)\left\{(1-e^2)[\log(1+e) - \log(1-e)] - 2e\right\}}$$

$$= \frac{2\sin \eta \cos \eta}{-2\sin^2 \eta} = -\cot \eta$$

unless $\eta = 0$ or π. Thus if terms of higher order than (b/a) are neglected, there is obtained, except for $\eta = 0$ or π,

$$V_r^*/V_o = -(b/a) \cot \eta \qquad (A7)$$

If it is remembered that the pressure coefficient at the surface of the spheroid is given by

$$P^* = 1 - (V_x^*/V_o)^2 - (V_r^*/V_o)^2$$

and if terms of higher order than $(b/a)^2$ are neglected it follows that

$$P^* = (b/a)^2 \log(b/a)^2 + (\cot^2 \eta + 2 - 2 \log 2)(b/a)^2 \qquad (A8)$$

unless $\eta = 0$ or π.

For some purposes it is convenient to give expressions for V_x^*/V_o, and P^* in terms of x instead of η in which case equations (A6) and (A8) become

$$\frac{V_x^*}{V_o} = 1 - \frac{1}{2}\left(\frac{b}{a}\right)^2 \log\left(\frac{b}{a}\right)^2 - \left(\frac{1}{1-(x/a)^2} - \log 2\right)\left(\frac{b}{a}\right)^2 \qquad (A9)$$

$$P^* = \left(\frac{b}{a}\right)^2 \log\left(\frac{b}{a}\right)^2 + \left(\frac{(x/a)^2}{1-(x/a)^2} + 2 - 2 \log 2\right)\left(\frac{b}{a}\right)^2 \qquad (A10)$$

REFERENCES

1. Ackeret, J.: Über Luftkräfte bei sehr grossen Geschwindigkeiten insbesondere bei ebenen Strömungen. Helvetica Physica Acta, vol. I, no. 5, 1928, pp. 301–322.

2. Glauert, H.: The Effect of Compressibility on the Lift of an Aerofoil. R. & M. No. 1135, British A.R.C., Sept. 1927.

3. Prandtl, L.: General Considerations on the Flow of Compressible Fluids. NACA TM No. 805, 1936.

4. Goldstein, S., and Young, A. D.: The Linear Perturbation Theory of Compressible Flow, with Applications to Wind-Tunnel Interference. R. & M. No. 1909, British A.R.C., 1943.

5. von Kármán, Th.: Compressibility Effects in Aerodynamics. Jour. Aero. Sci., vol. 8, no. 9, July 1941, pp. 337–356.

6. Robinson, Russell G., and Wright, Ray H.: Estimation of Critical Speeds of Airfoils and Streamline Bodies. NACA ACR, March 1940. (Classification cancelled.)

7. Wright, Ray H.: Estimation of Pressures on Cockpit Canopies, Gun Turrets, Blisters, and Similar Protuberances. NACA ACR No. L4E10, 1944. (Classification cancelled.)

8. Göthert, B.: Ebene und räumliche Strömung bei hohen Unterschallgeschwindigkeiten (Erweiterung der Prandtlschen Regel). Lilienthal-Gesellschaft für Luftfahrtforschung, Bericht 127, Sept. 1940, pp. 97–101.

9. Schmieden, C., und Kawalki, K. H.: Beiträge zum Umströmungsproblem bei hohen Geschwindigkeiten, II. Teil, Einfluss der Kompressibilität bei rotationssymmetrischer Umströmung eines Ellipsoids. Lilienthal-Gesellschaft für Luftfahrtforschung, Bericht S 13/1 Teil, 1942, pp. 48–68. See also Deutsche Luftfahrtforschung Forschungsbericht Nr. 1633, 1942.

10. Wieselsberger, C.: Über den Einfluss der Windkanalbegrenzung auf den Widerstand insbesondere im Bereiche der kompressiblen Strömung. Luftfahrtforschung, vol. 19, no. 4, May 6, 1942, pp. 124–128.

11. Abbott, Ira H.: Fuselage-Drag Tests in the Variable-Density Wind Tunnel: Streamline Bodies of Revolution, Fineness Ratio of 5. NACA TN No. 614, 1937.

12. Brand, M.: Druckverteilungen von Rotationskörpern bei achsialer Anströmung. Deutsche Luftfahrtforschung Untersuchungen und Mitteilungen Nr. 3206, 1944.

13. Bilharz, H., und Hölder, E.: Zur Berechung der Druckverteilung an Rotationskörpern in der Unterschallströmung eines Gases. Teil I: Achsensymmetrische Strömung. Deutsche Luftfahrtforschung Forschungsbericht Nr. 1169/1, Jan. 1940.

14. Delano, James B.: Pressure Distribution on the Fuselage of a Mid-wing Airplane Model at High Speeds. NACA TN No. 890, 1943.

15. Lamb, Horace: Hydrodynamics. Cambridge Univ. Press, 6th ed., 1932.

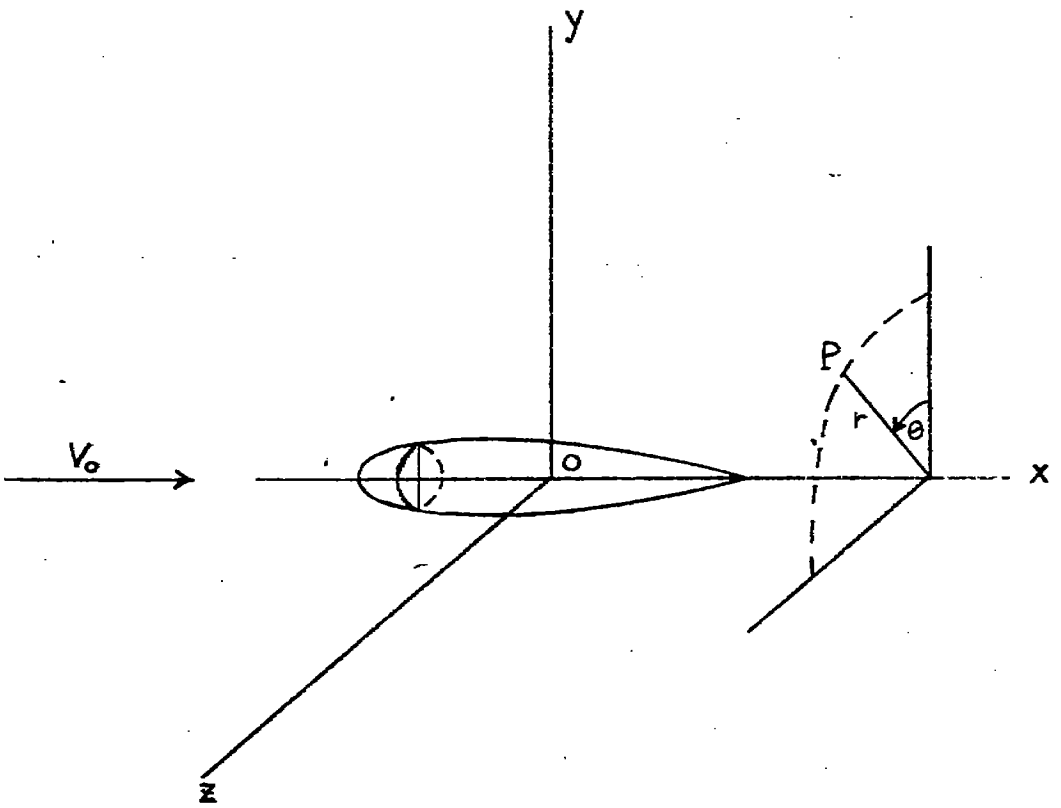

NATIONAL ADVISORY COMMITTEE
FOR AERONAUTICS

FIGURE 1.— DIAGRAM SHOWING POSITION OF ARBITRARY BODY OF REVOLUTION RELATIVE TO COORDINATE SYSTEMS.

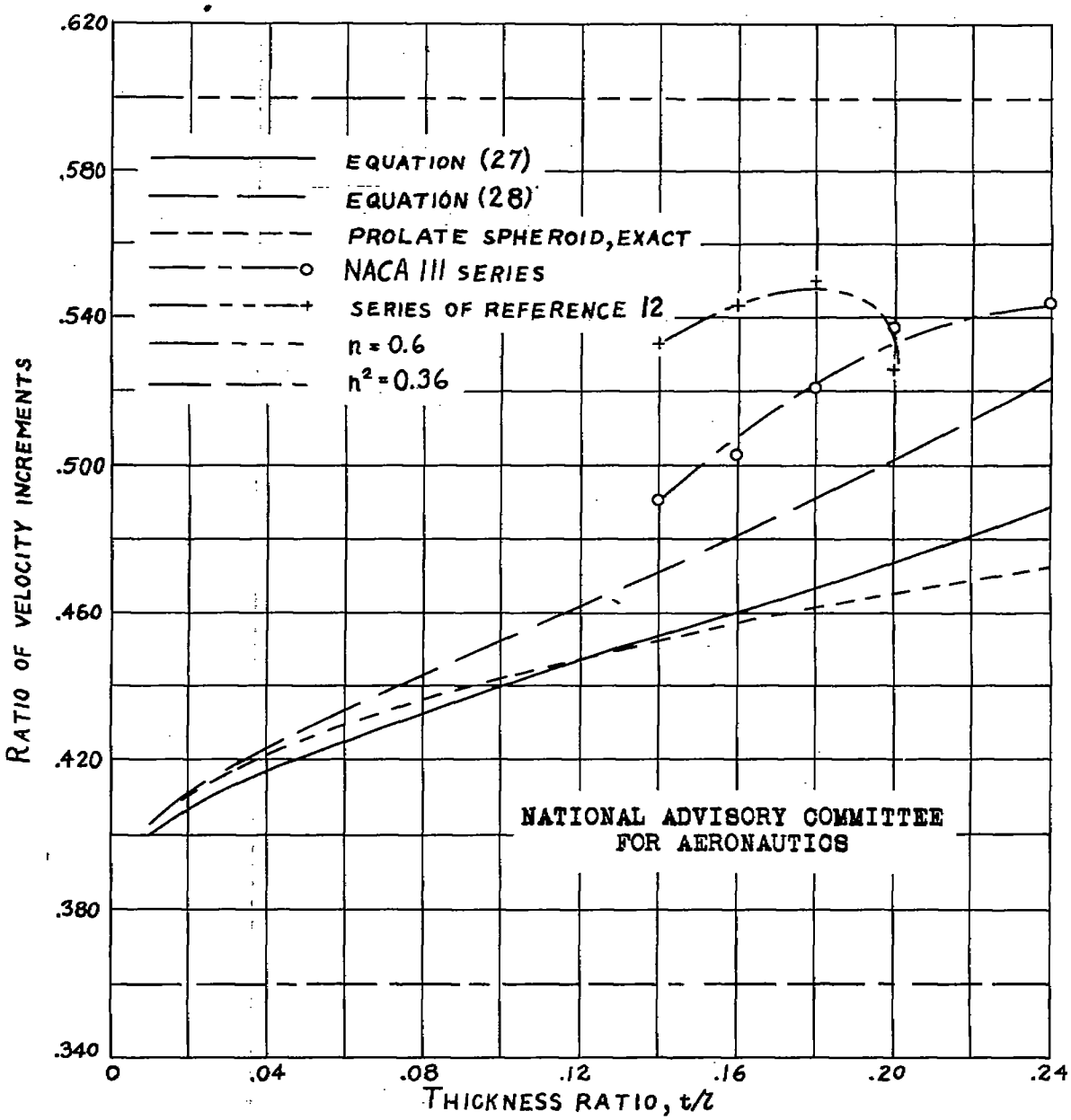

FIGURE 2.- RATIO OF MAXIMUM VELOCITY INCREMENTS FOR TWO BODIES WHOSE THICKNESSES ARE IN THE RATIO 0.6 TO 1 AS A FUNCTION OF THE THICKNESS RATIO OF THE THICKER BODY.

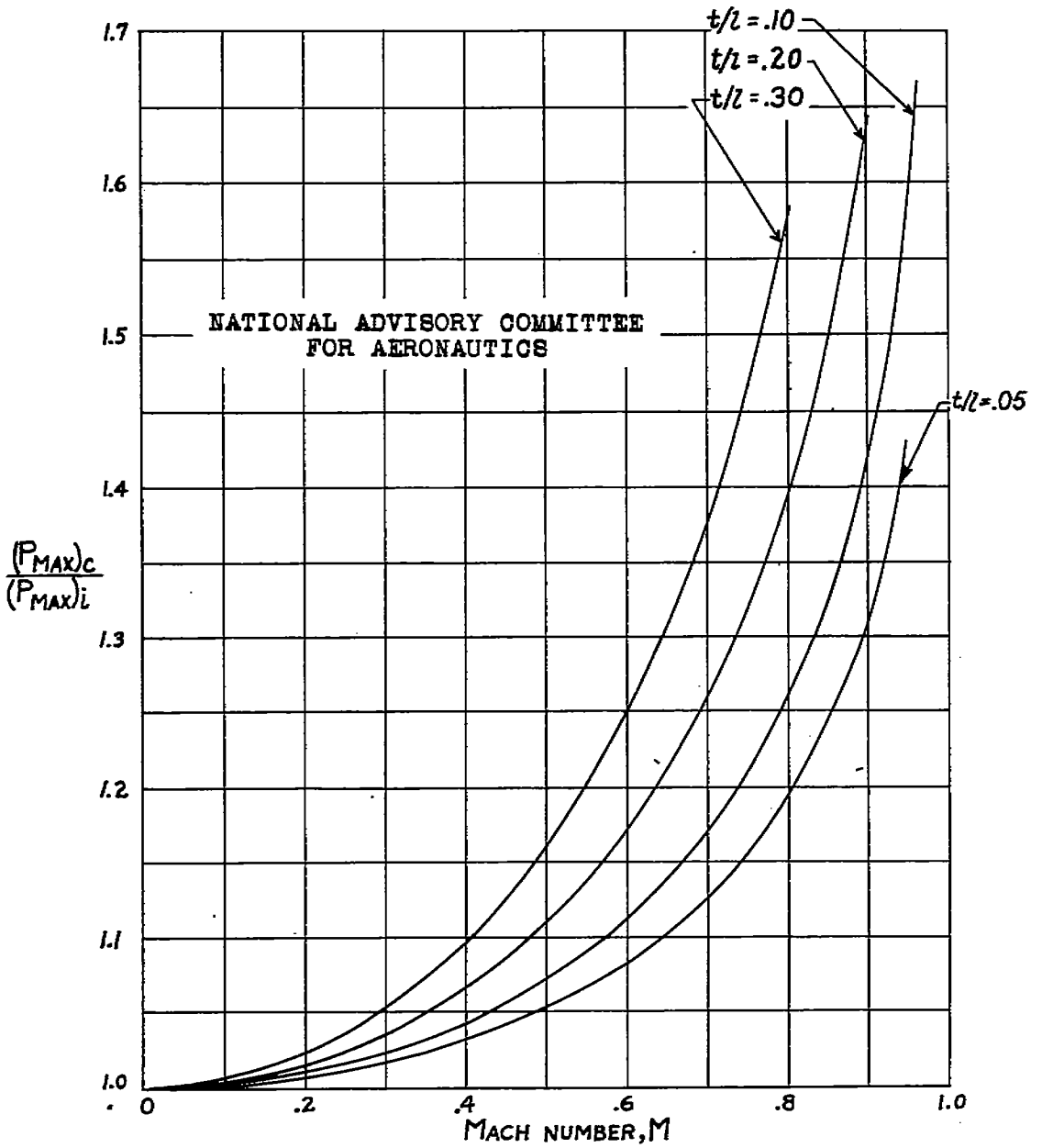

FIGURE 3.- VARIATION OF $(P_{MAX})_c/(P_{MAX})_i$ WITH MACH NUMBER FOR VARIOUS THICKNESS RATIOS. (EQUATION (30).)

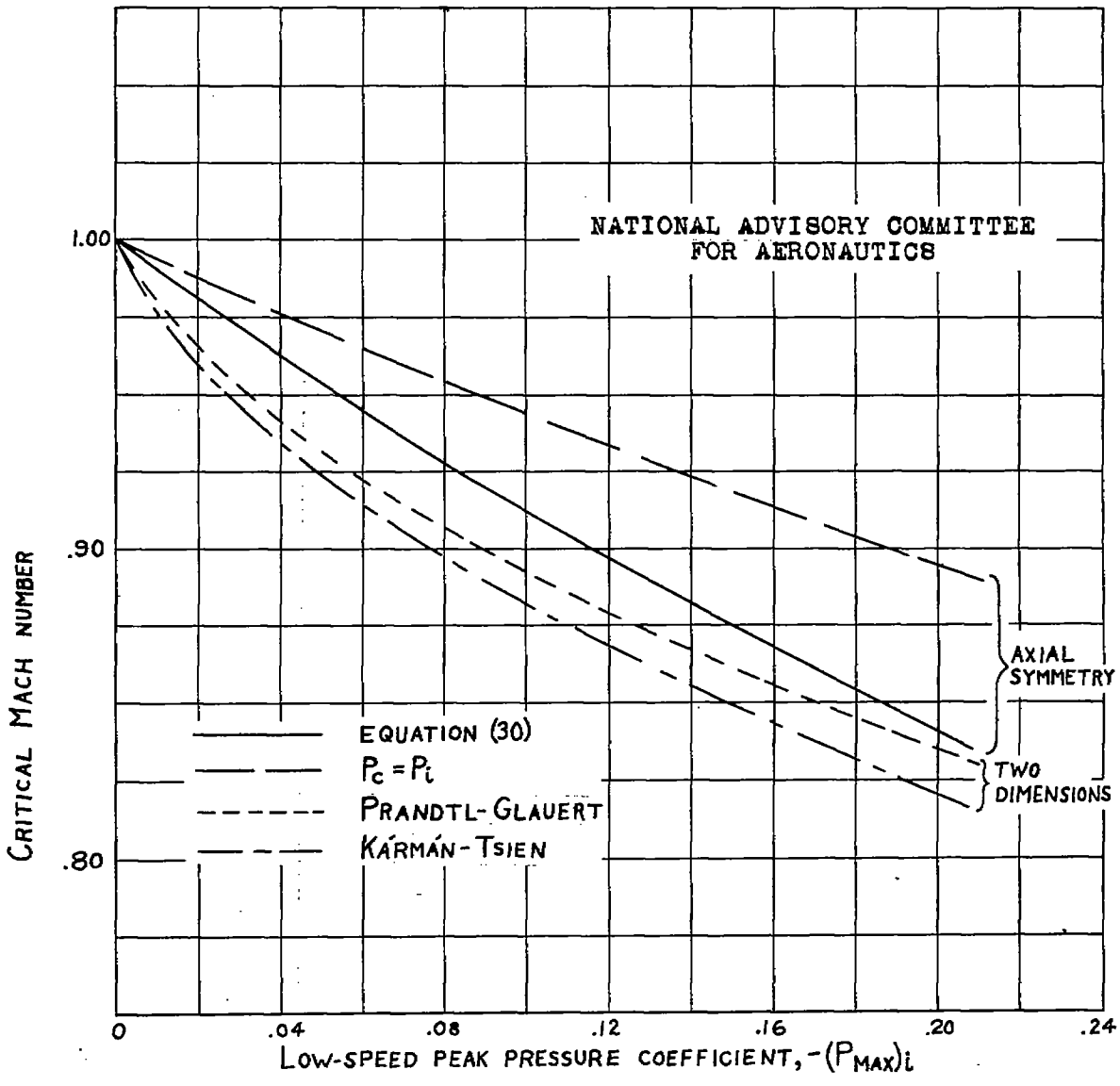

FIGURE 4.- CRITICAL MACH NUMBER CHART.

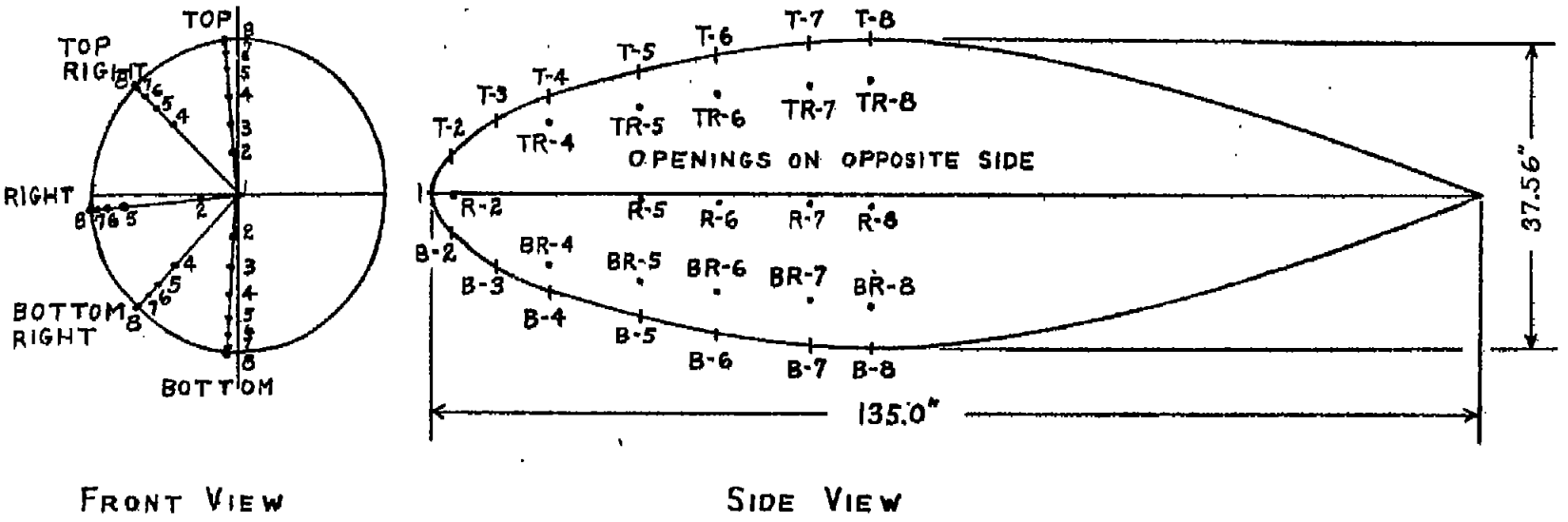

FRONT VIEW

SIDE VIEW

NATIONAL ADVISORY COMMITTEE
FOR AERONAUTICS

FIGURE 5.- LOCATION OF PRESSURE ORIFICES ON MODEL OF FUSELAGE OF AIRPLANE A.

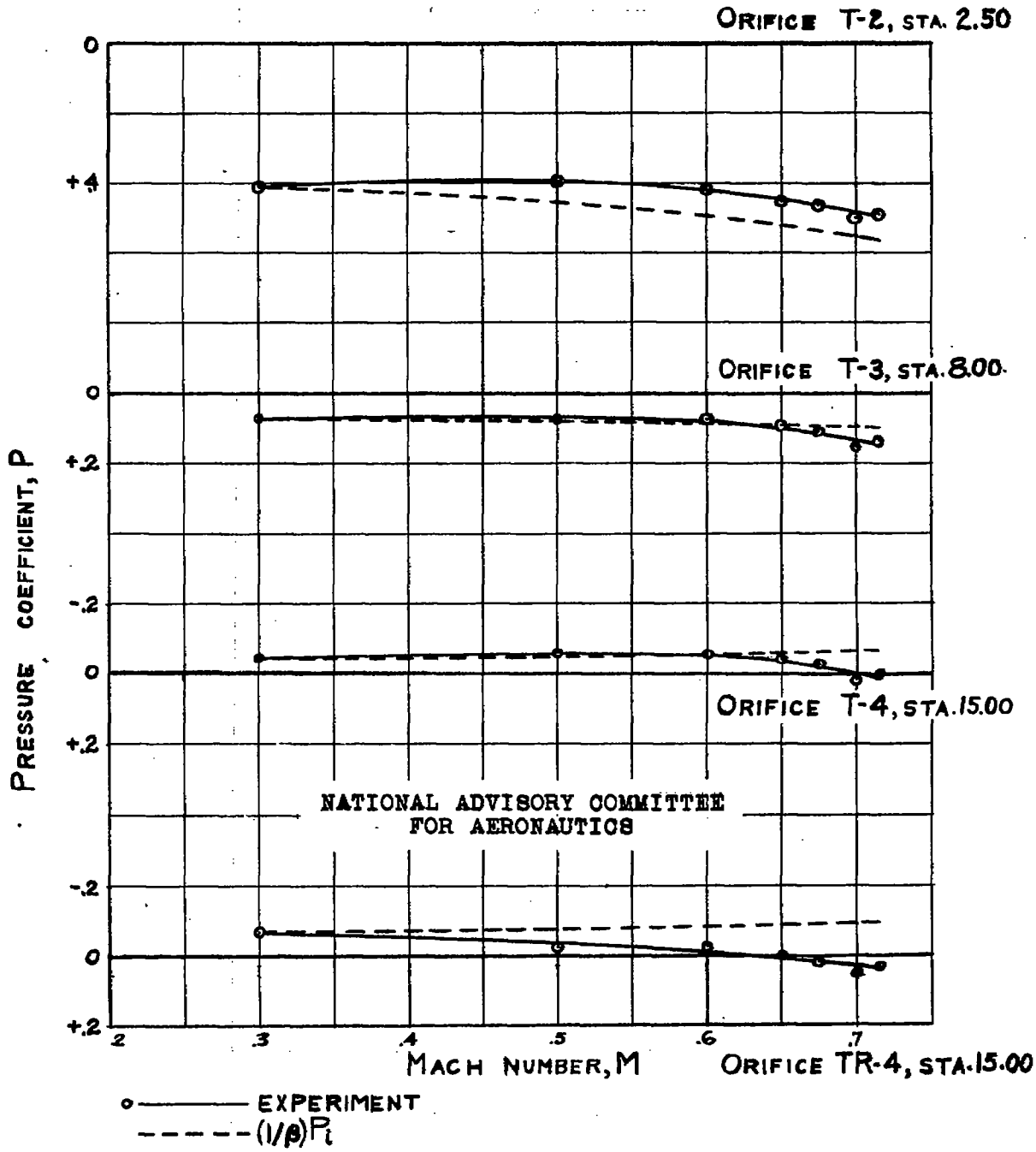

(a) ORIFICES T-2, T-3, T-4, TR-4.

FIGURE 6.- VARIATION OF PRESSURE COEFFICIENT WITH MACH NUMBER ON MODEL OF FUSELAGE OF AIRPLANE A. α, 0°.

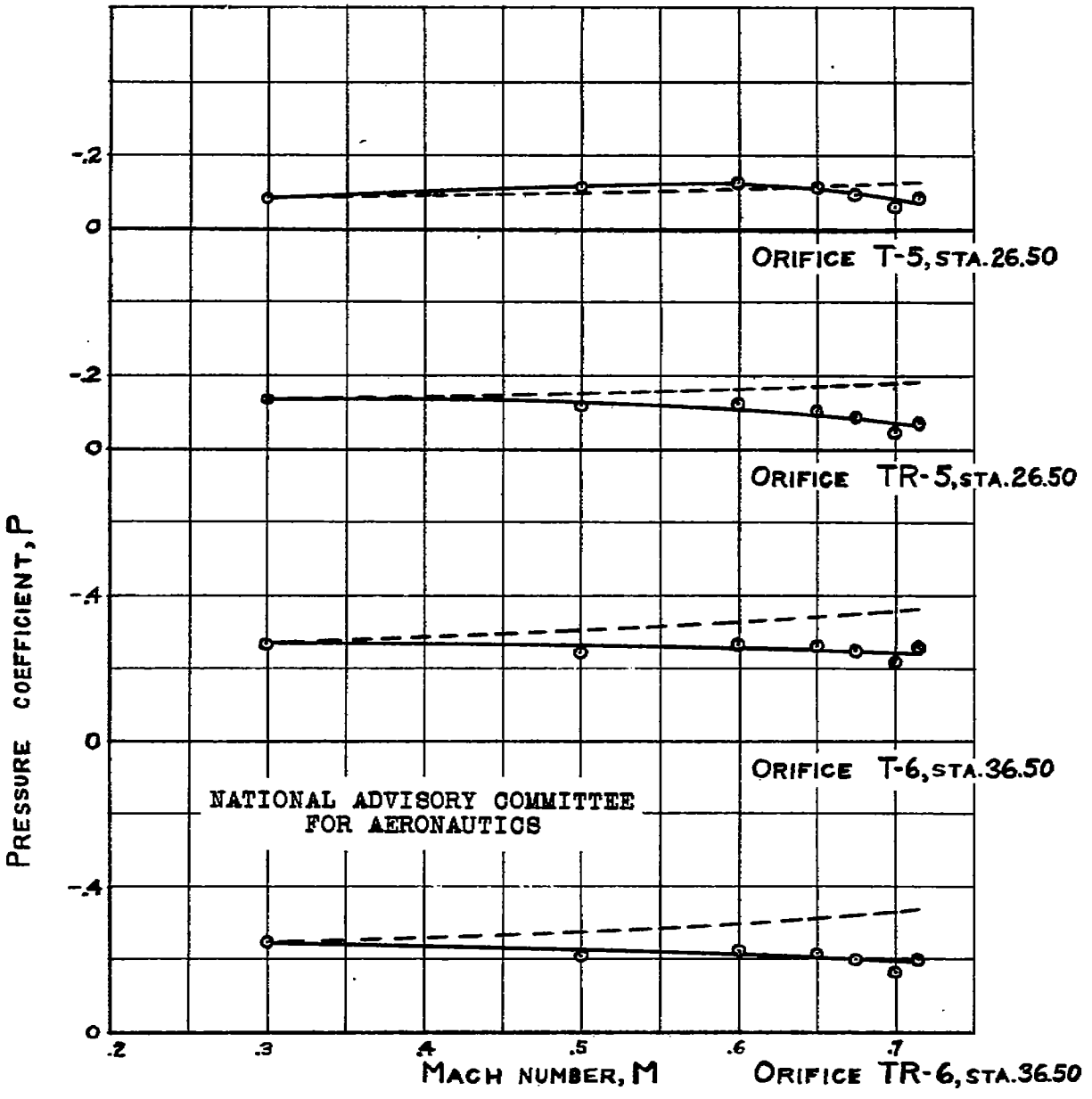

(b) ORIFICES T-5, TR-5, T-6, TR-6.

FIGURE 6.- CONTINUED. VARIATION OF PRESSURE COEFFICIENT WITH MACH NUMBER ON MODEL OF FUSELAGE OF AIRPLANE A. α, 0°.

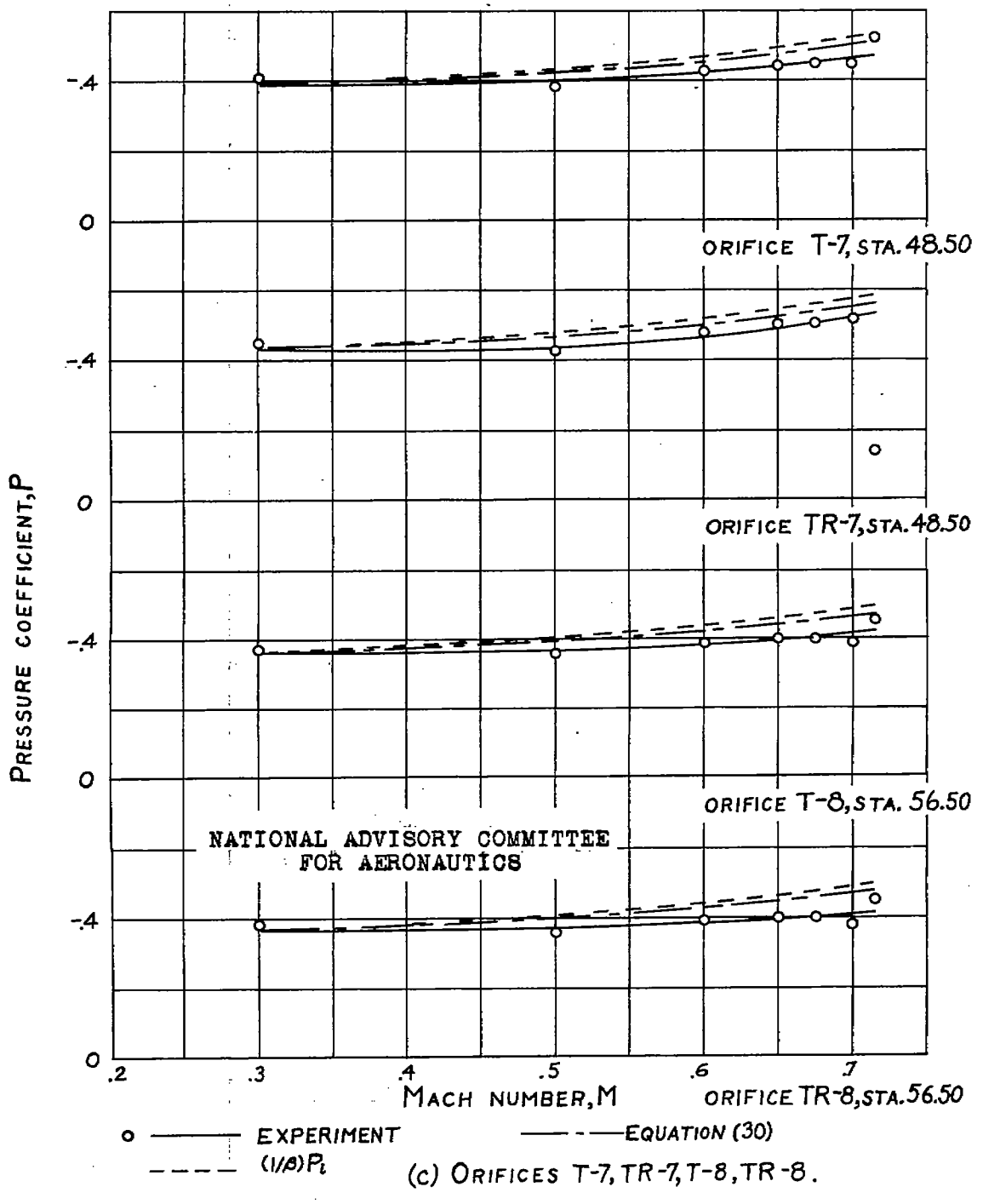

(c) Orifices T-7, TR-7, T-8, TR-8.

FIGURE 6. - CONCLUDED. VARIATION OF PRESSURE COEFFICIENT WITH MACH NUMBER ON MODEL OF FUSELAGE OF AIRPLANE A. α, 0°.

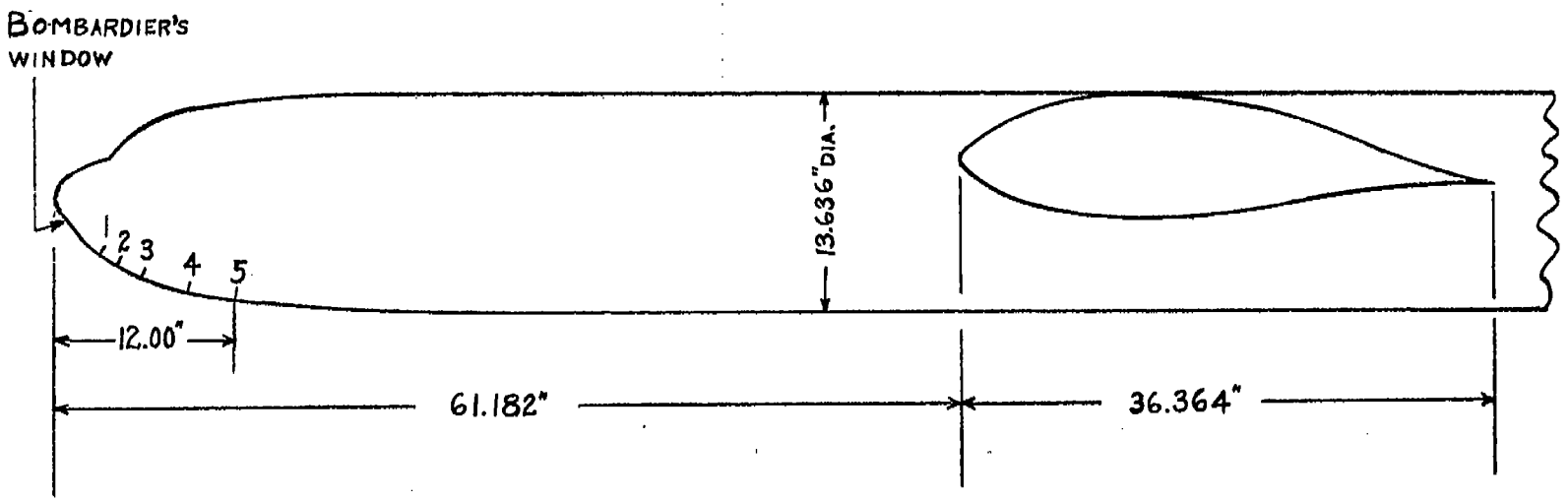

NATIONAL ADVISORY COMMITTEE
FOR AERONAUTICS

FIGURE 7.- LOCATION OF PRESSURE ORIFICES NEAR NOSE ON FUSELAGE OF 1/11-SCALE MODEL OF AIRPLANE B.

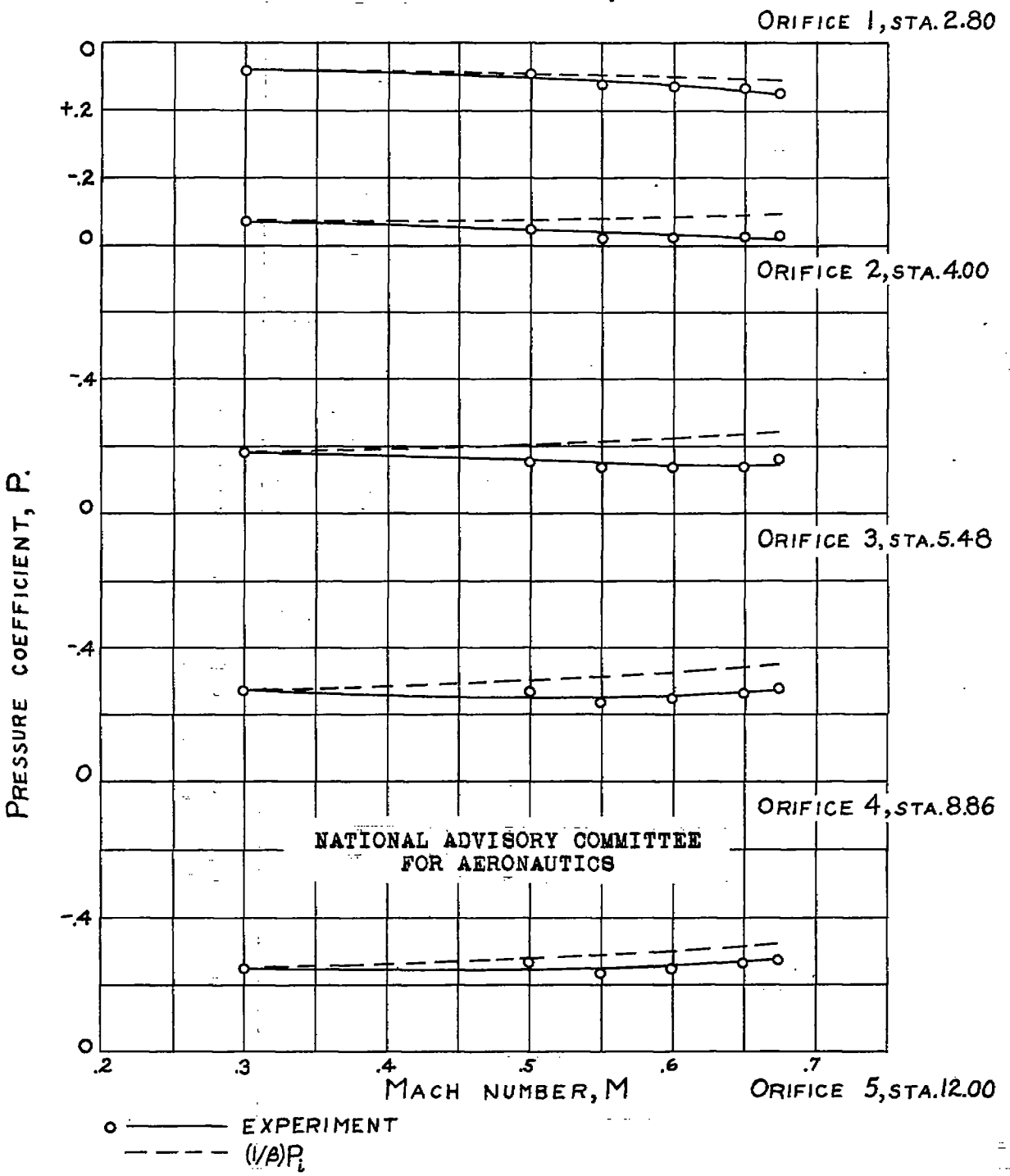

FIGURE 8.- VARIATION OF PRESSURE COEFFICIENT WITH MACH NUMBER AT FIVE LOWER SURFACE STATIONS ON VERTICAL CENTER LINE OF FUSELAGE OF 1/11-SCALE MODEL OF AIRPLANE B. α, 0°.

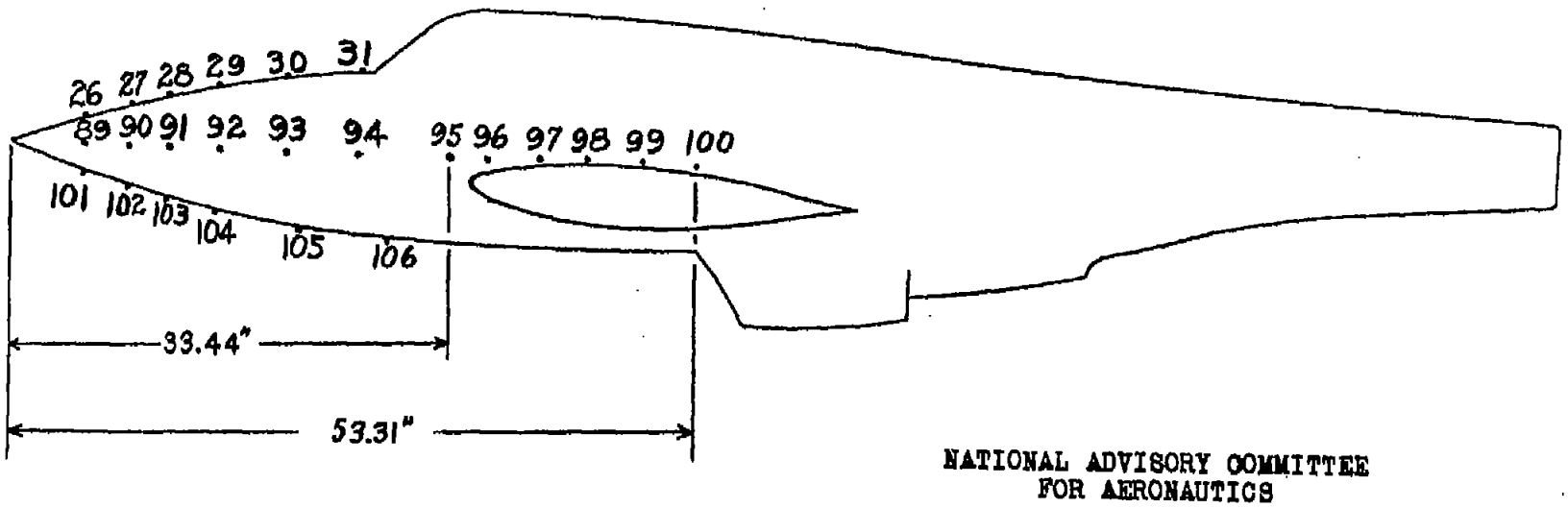

FIGURE 9.- LOCATION OF PRESSURE ORIFICES ON FUSELAGE OF 1/5-SCALE MODEL OF WING, FUSELAGE, AND CANOPY OF AIRPLANE C.

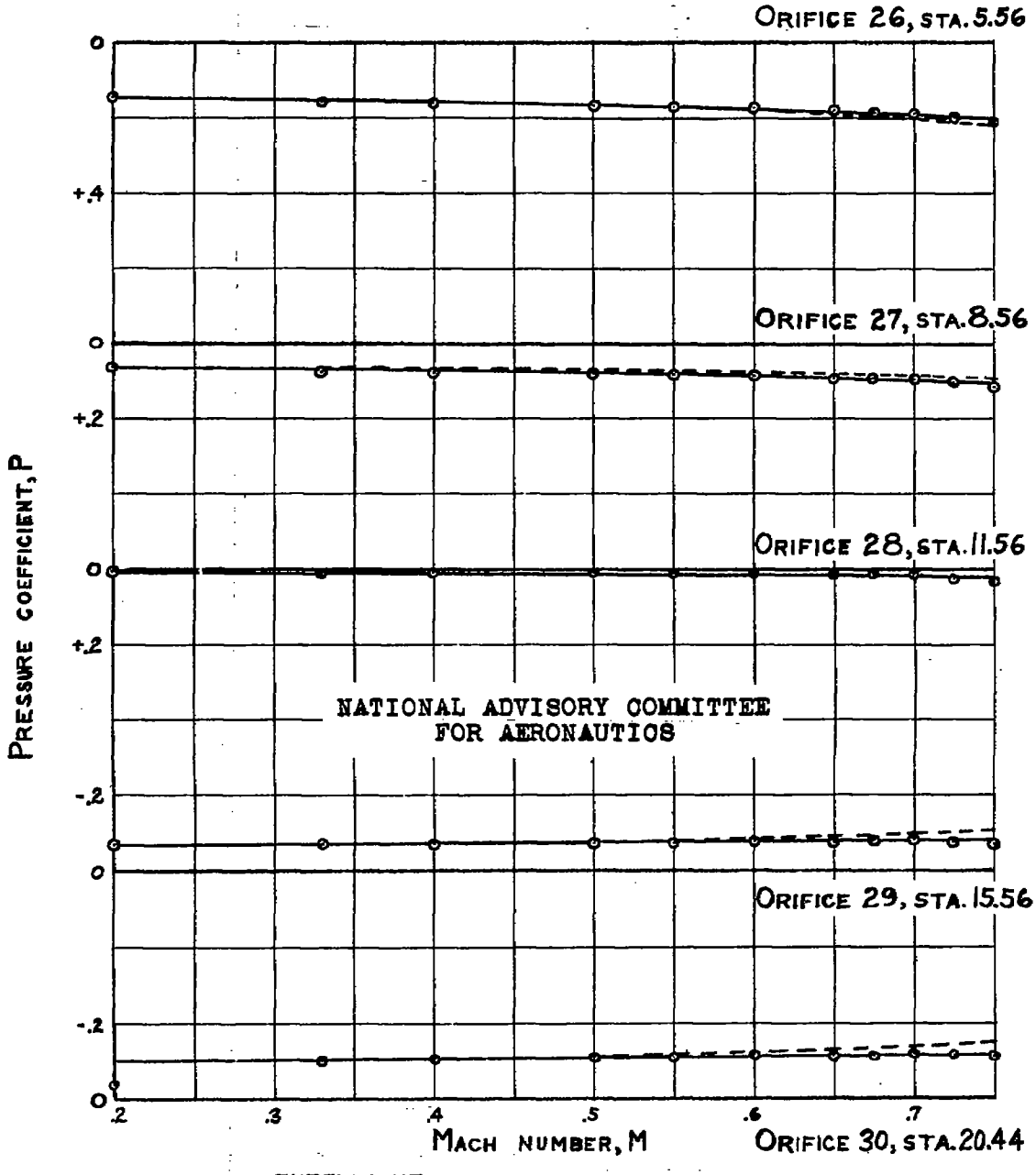

(a) Top orifices 26, 27, 28, 29, 30.

FIGURE 10. - VARIATION OF PRESSURE COEFFICIENT WITH MACH NUMBER ON BASIC FUSELAGE FOR WING AND BASIC FUSELAGE OF 1/5-SCALE MODEL OF AIRPLANE C. α, -0.25°.

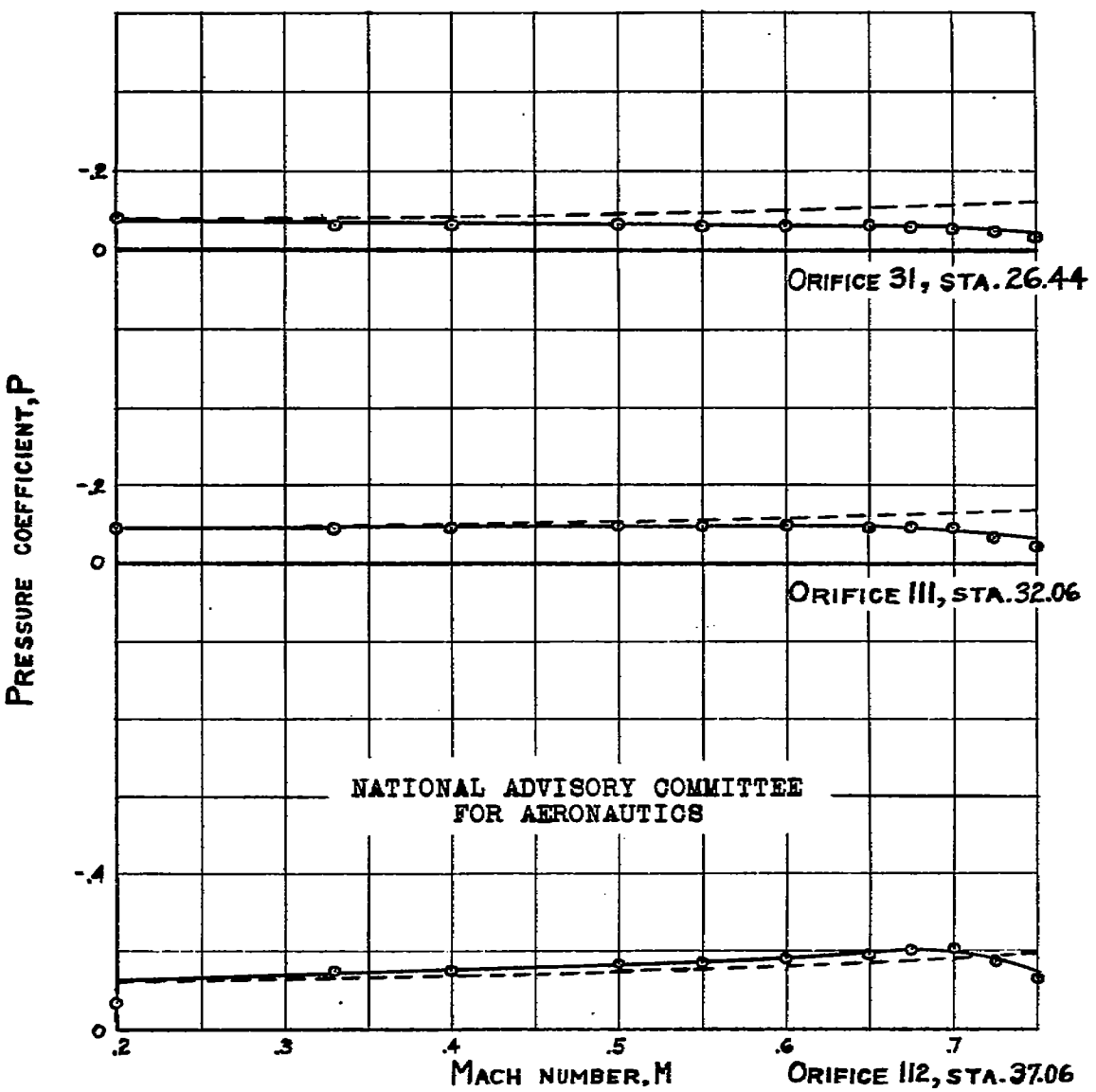

(b) Top orifices 31, 111, 112.

Figure 10.- Continued. Variation of pressure coefficient with Mach number on basic fuselage for wing and basic fuselage of 1/5-scale model of airplane C. α,-0.25°.

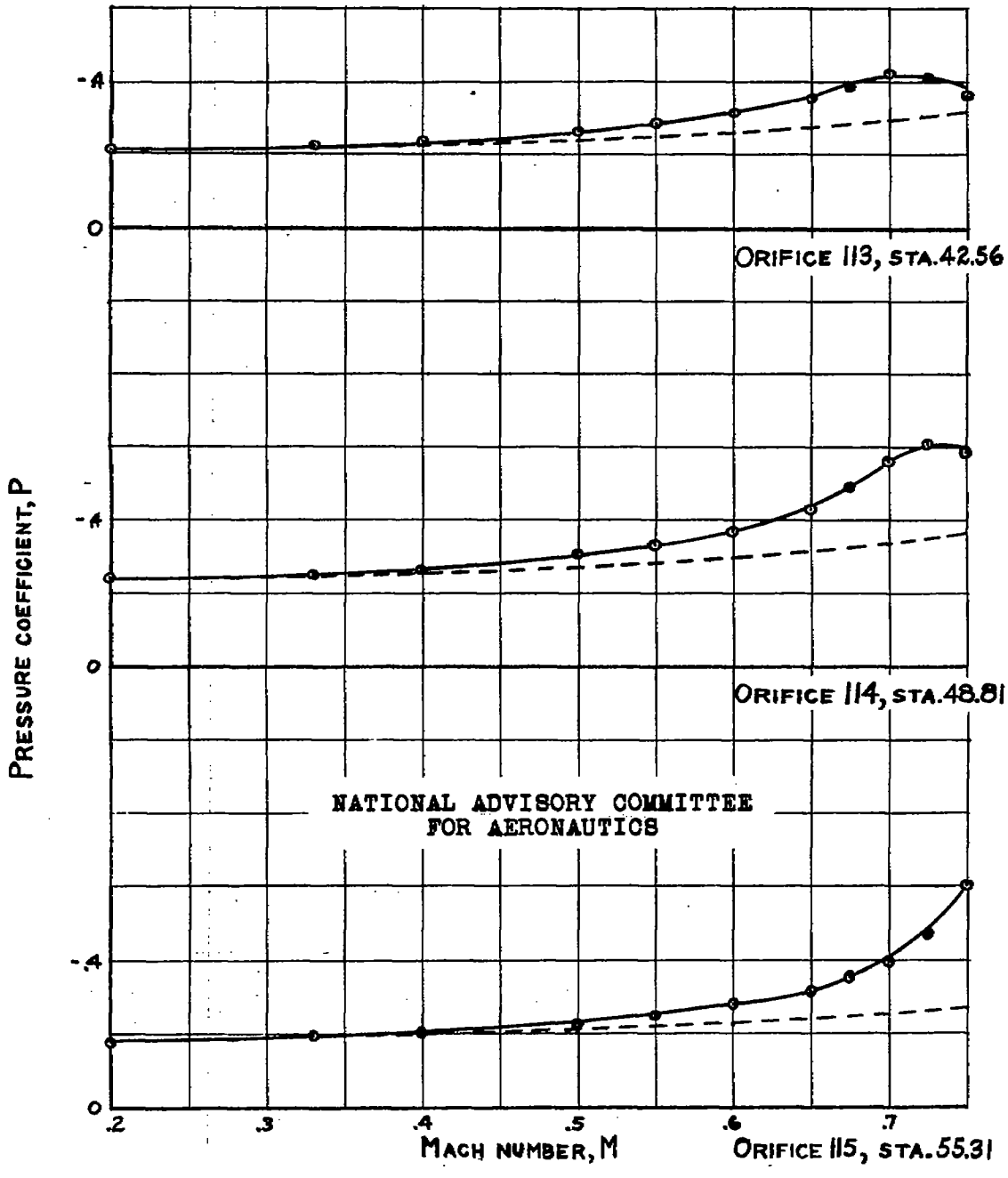

(c) Top orifices 113, 114, 115.

Figure 10.- Continued. Variation of pressure coefficient with Mach number on basic fuselage for wing and basic fuselage of 1/5-scale model of airplane C. α_s -0.25°.

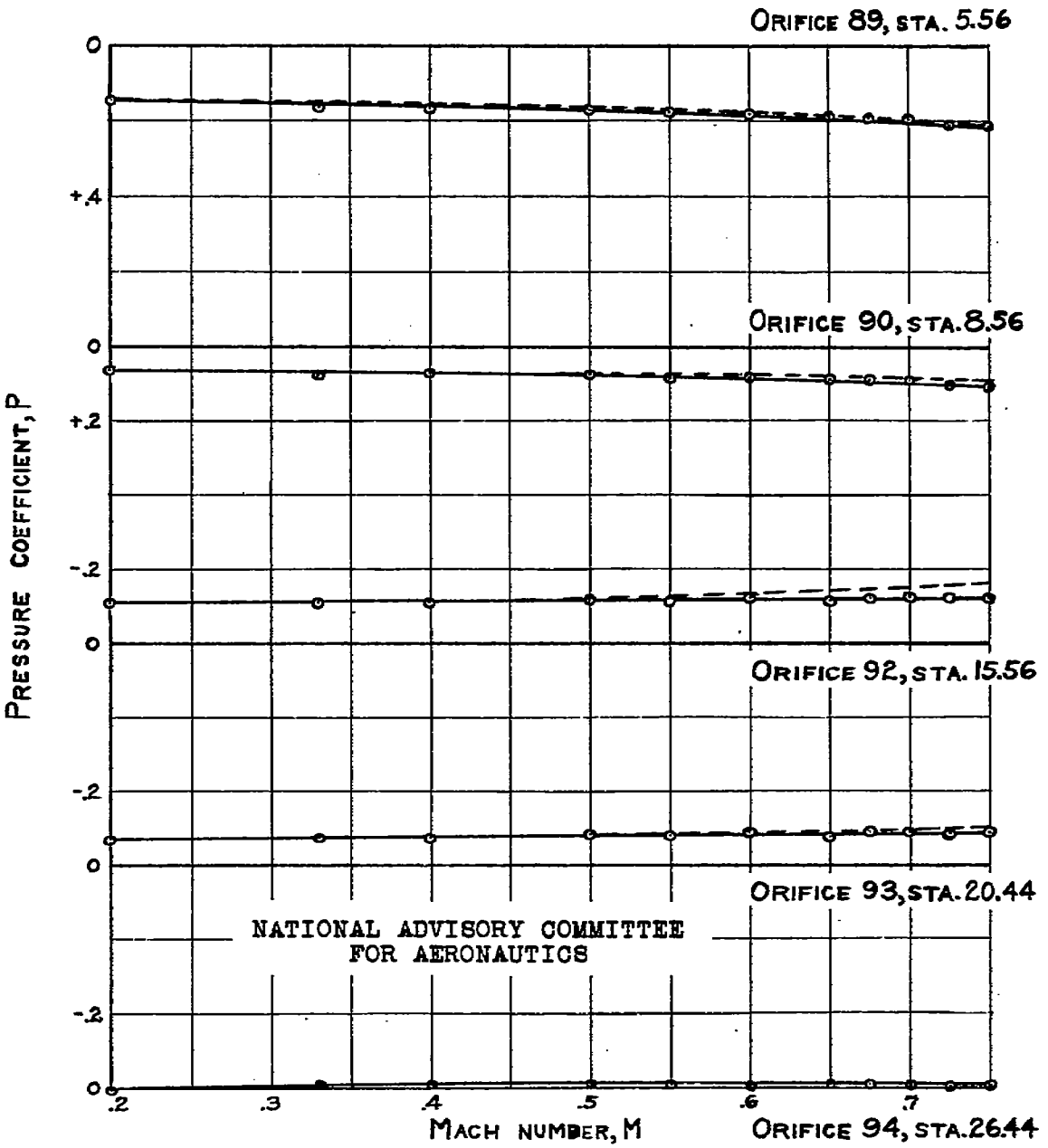

(d) Side orifices 89, 90, 92, 93, 94.

FIGURE 10.- CONTINUED. VARIATION OF PRESSURE COEFFICIENT WITH MACH NUMBER ON BASIC FUSELAGE FOR WING AND BASIC FUSELAGE OF 1/5-SCALE MODEL OF AIRPLANE C. α, -0.25°.

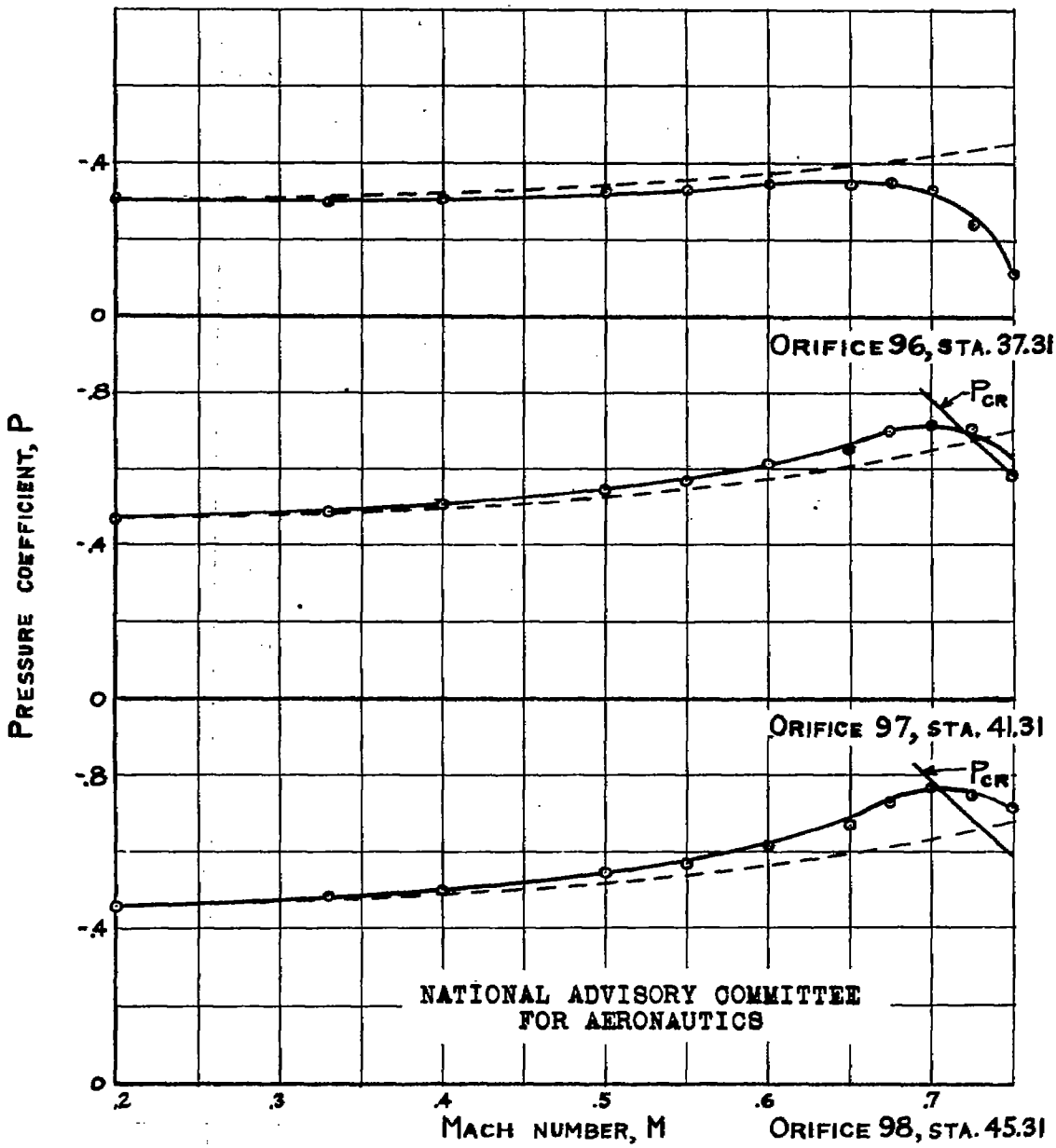

(e) SIDE ORIFICES 96, 97, 98.

FIGURE 10.- CONTINUED. VARIATION OF PRESSURE COEFFICIENT WITH MACH NUMBER ON BASIC FUSELAGE FOR WING AND BASIC FUSELAGE OF 1/5-SCALE MODEL OF AIRPLANE C. α, -0.25°

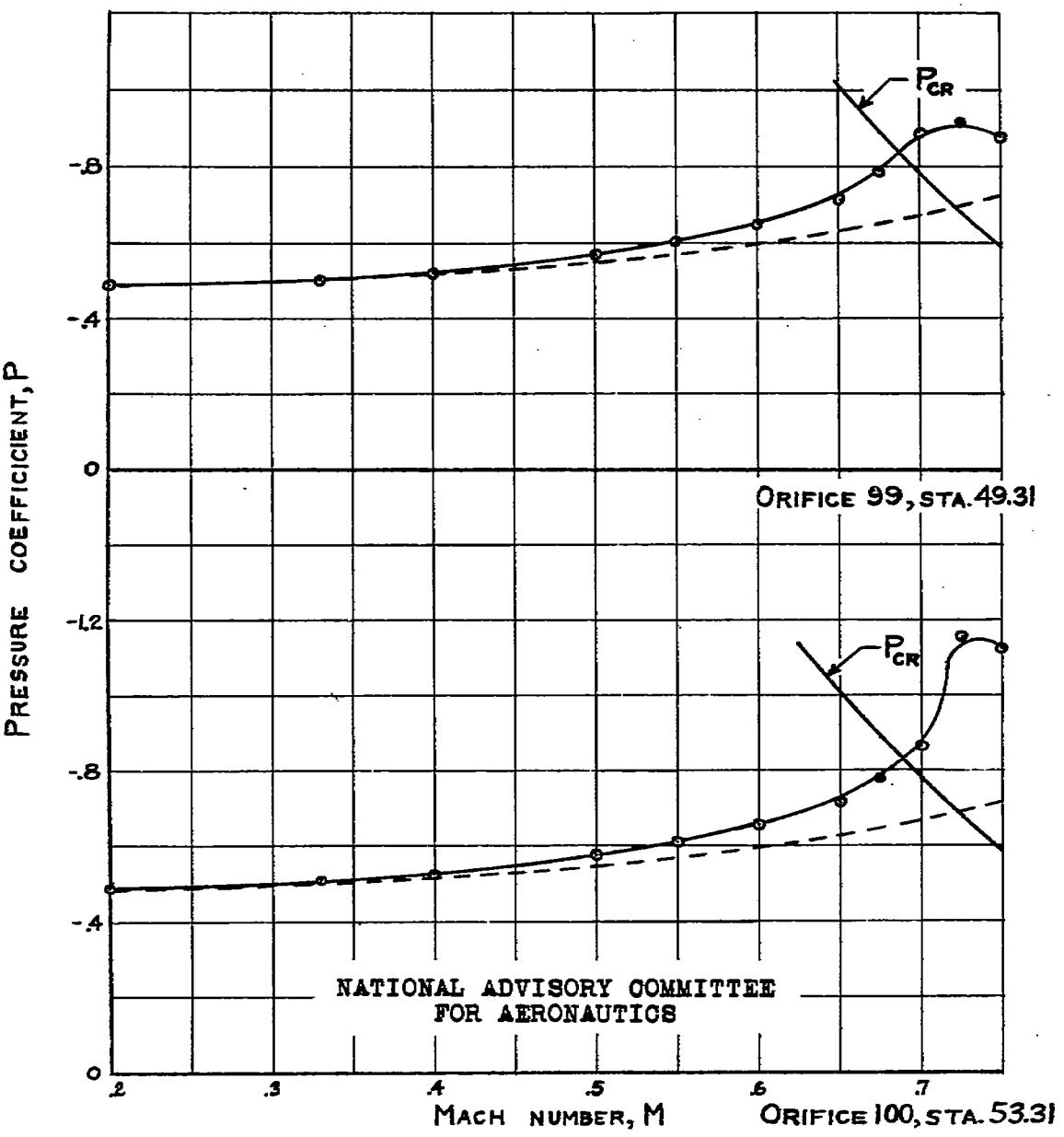

(f) SIDE ORIFICES 99, 100.

FIGURE 10.- CONTINUED. VARIATION OF PRESSURE COEFFICIENT WITH MACH NUMBER ON BASIC FUSELAGE FOR WING AND BASIC FUSELAGE OF 1/5-SCALE MODEL OF AIRPLANE C. α, -0.25°

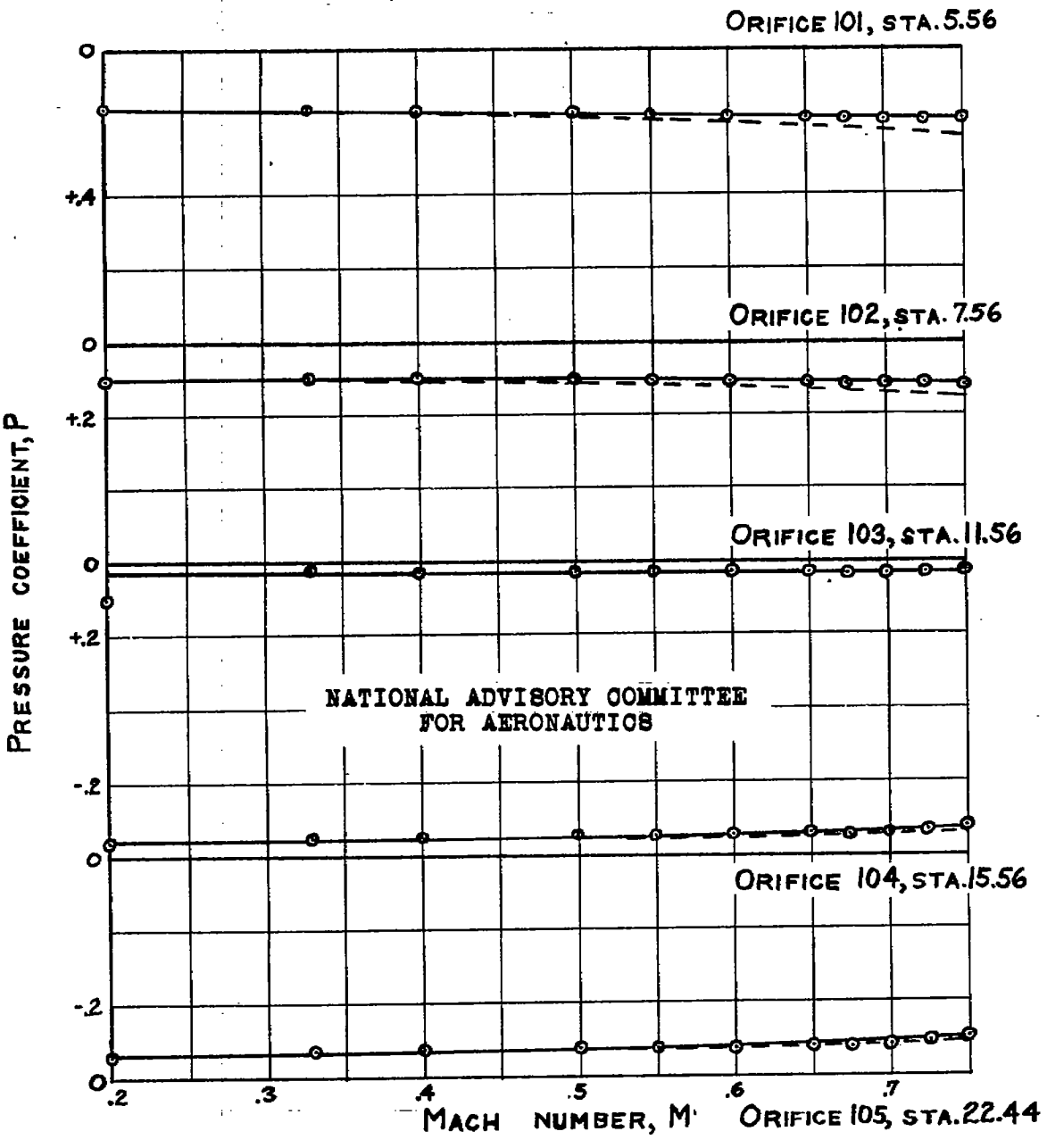

(g) Bottom orifices 101,102,103,104,105.

FIGURE 10.- CONTINUED. VARIATION OF PRESSURE COEFFICIENT WITH MACH NUMBER ON BASIC FUSELAGE FOR WING AND BASIC FUSELAGE OF 1/5-SCALE MODEL OF AIRPLANE C. α,-0.25°

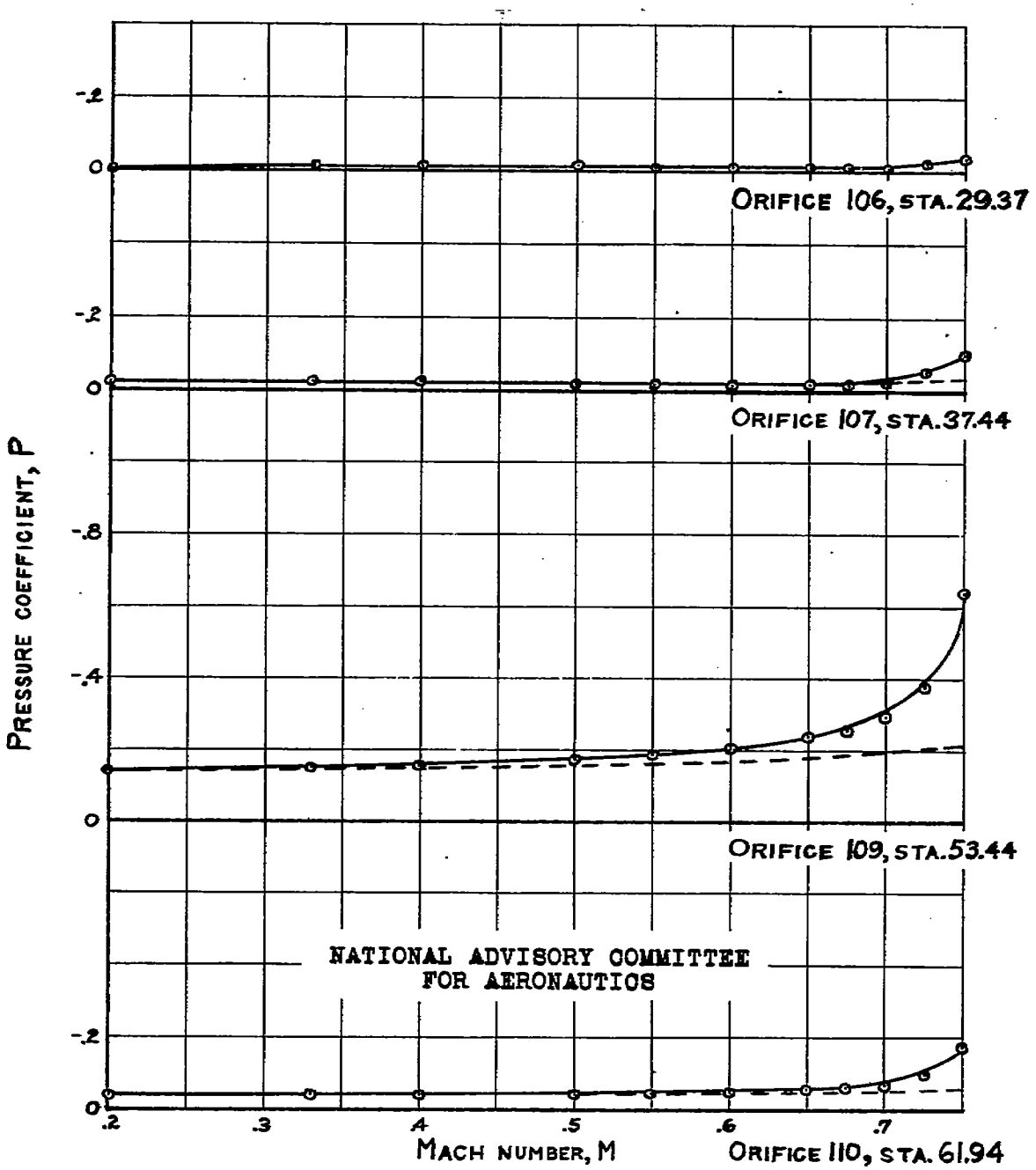

(h) Bottom orifices 106, 107, 109, 110.

FIGURE 10.- Concluded. Variation of pressure coefficient with Mach number on basic fuselage for wing and basic fuselage of 1/5-scale model of airplane C. α, -0.25°

Figure 11.- Kollsman pitot-static tube F.S.S.C. No. 88-T-2950.

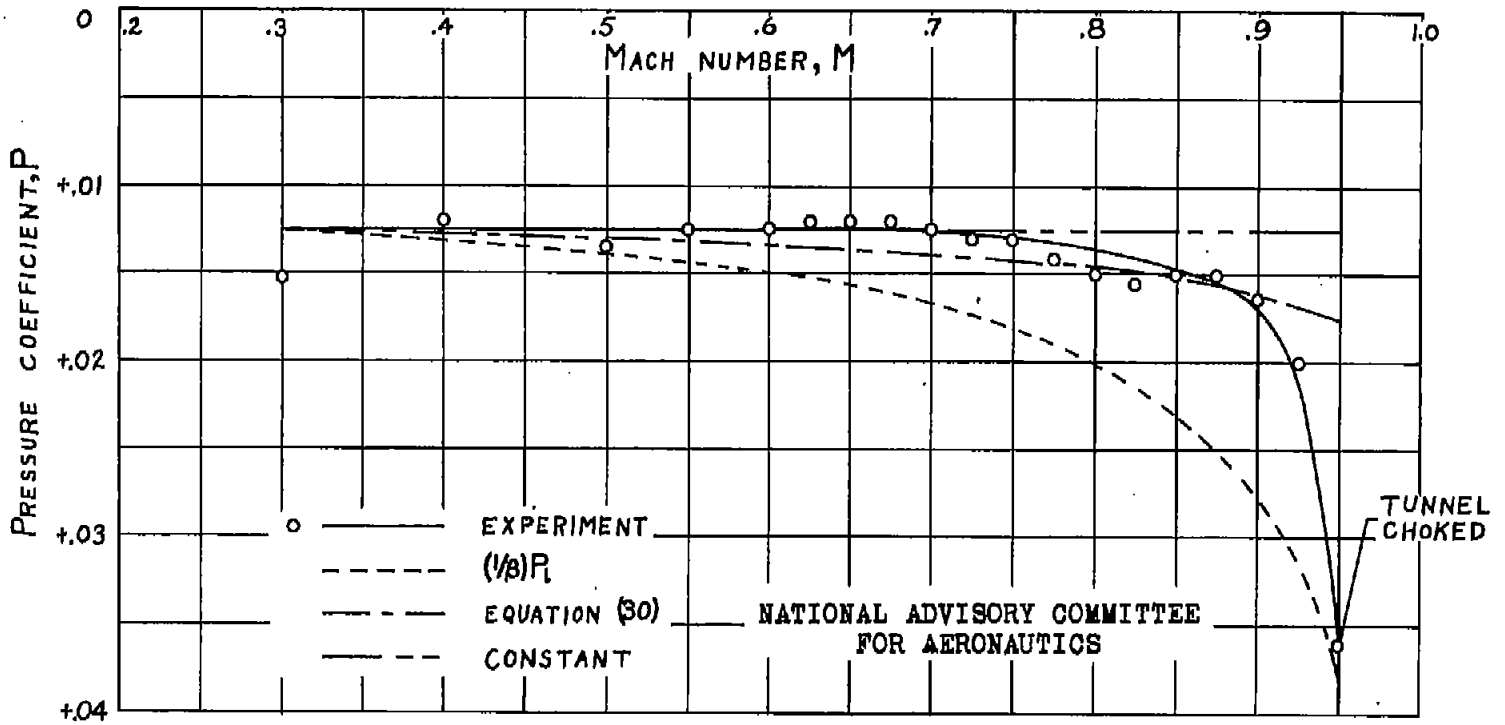

FIGURE 12.- VARIATION OF PRESSURE COEFFICIENT WITH MACH NUMBER AT STATIC ORIFICES OF KOLLSMAN PITOT-STATIC TUBE F.S.S.C. No. 88-T-2950. PITCH, 0°; YAW 0°.